ACCELERATOR NEUTRINO EXPERIMENTS

D.H. Perkins

Department of Nuclear Physics,
Oxford, England.

This talk is divided into two parts. In the first part, I consider the properties of the purely leptonic weak currents, as measured with neutrino beams; these have been the subject of much theoretical speculation, perhaps not unconnected with the meagreness of the experimental information available. In the second part I discuss some of the semileptonic interactions, involving the weak hadron currents, for which the data is somewhat more abundant and the comparison with theory more definite.

1. LEPTONIC INTERACTIONS

1.1 Lepton conservation

In the 1967 CERN experiments, Borer et al [1] determined the ratio of positive to negative muons in a magnetized iron spark chamber exposed to the improved CERN ν - beam. They observed

$$N\mu^+ / N\mu^- = 7/2730$$

The focussing system was set to focus positive pions and kaons (decaying to $\nu\mu$) and defocus negatives (giving $\overline{\nu}\mu$). The observed μ^+ events could all be accounted for in terms of various backgrounds, including $\overline{\nu}\mu$ background. The level of possible non-conservation of leptons, at 95% confidence level, is

$$\frac{\nu\mu \rightarrow \mu^+}{\nu\mu \rightarrow \mu^-} < 4.6.10^{-3}$$

The improvement over the previous limit [2] of $< 1.5.10^{-2}$ is largely a result of the improved focussing properties of the 3-stage, as compared with the old 1 - stage, beam.

1.2 Intermediate Boson W.

An important question is to what extent the new multi-100 GeV accelerators will extend the limit on Mw. In the past, searches have been made for

evidence of boson production in both strong interactions and with neutrino beams.

In the experiment of Burns et al [3] at BNL, a 20-30 GeV proton beam was incident on a thick shield, and observations made on energetic muons emerging at wide angle. The transverse momentum distribution from pion and kaon decay falls off exponentially (as exp $(-p_T/0.2)$ at large p_T, so that the decay of a heavy particle $W \rightarrow \mu + \nu$ might appear as an anomaly in the distribution, for p_T of the order of GeV. Of course, processes other than W production could contribute extra wide-angle muons. In any case no signal was observed and the limit on the W - production cross section was

$$\sigma_W \cdot B \leqslant 4.10^{-34} \text{ cm}^2/\text{nucleon}$$

where B is the branching ratio $W \rightarrow \mu + \nu / W \rightarrow$ anything. The experiment was sensitive to the mass range $2 < Mw < 6$ Gev. Unfortunately, since there is no reliable way of estimating σ_W theoretically, it is hard to draw any conclusions from this negative result.

Using neutrino beams, electromagnetic production of W would take place by the process of Fig. 1.

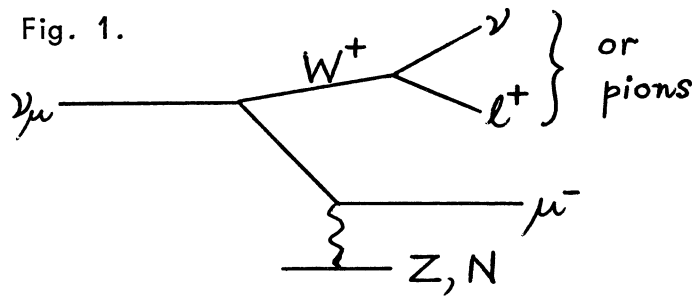

Fig 1.

The expected cross-sections can be calculated reliably, the only unknowns being the boson mass and g-factor. Assuming g = 1- and other values do not give widely different results - the conclusions of the CERN and BNL experiments, irrespective of branching ratios, can be summarized as follows:-

Proton Energy			Decay Mode	
30 GeV	BNL	SC	$W \rightarrow e + \nu$	$M_W > 1.8$ GeV (99% confidence)
24 GeV	CERN	SC	$W \rightarrow \mu + \nu$	
24 GeV	CERN	BC	$W \rightarrow \pi$'s	

Fig. 2 shows the approximate boson production rates predicted for different proton energies, assuming an optimized 3-element focussing system, as scaled up from the present CERN arrangement, and for detectors of medium atomic weight (Al). The curves were extrapolated from the computations of Wu et al [4], carried out for values of M_W up to 2.5 GeV and E_ν up to 20 GeV. The horizontal dotted line indicates the level of the CERN/BNL experiments of 1963/64 and probably gives a fair estimate of the mass limits which could be reached at higher energies, for the following reasons. Fig. 3 indicates the expected boson rates as well as the total inelastic rate for an experiment at 75 GeV (Serpukhov). The frequency and multiplicity of the inelastic background increases with neutrino energy, and the leptonic decay branching ratio probably decreases at high Mw. On the other hand the signal/noise ratio of the $\mu+\mu-$ signature associated with the muonic decay mode improves exponentially with the muon range, and hence neutrino energy.

So, while one could not hope, just by using more intense beams or greater detector mass, to improve substantially the limit on Mw at 20 - 30 GeV machines, it appears fairly clear that the W-boson could be observed using a 300 GeV accelerator, if the mass were less than 8 GeV. Several theoretical extimates of the mass have appeared. For example, Glashow et al [5] estimate $M_W \sim 8$ GeV from the $K\pi 2$ decay rate, using current algebra. Mohapatra et al [6] and Gell Mann et al [7] give $M_W \sim 3$-4 GeV, from a calculation of the $K_L - K_S$ mass difference, if one interprets M_W as an effective cut-off in a perturbation calculation.

1.3 Diagonal Interactions

The problems encountered in attempting to arrive at a renormalizeable theory of weak interactions are well known. The present working hypothesis (due to Fermi) consists of keeping only the lowest-order term, which term however diverges quadratically at high energy (e.g. neutrino-electron elastic scattering). A cut-off can be imposed to preserve unitarity, but then higher-order terms are of the same magnitude as the first and the result of summing all graphs is still divergent. Many cures have been proposed, generally invoking large numbers of different scalar and vector bosons, heavy leptons or other

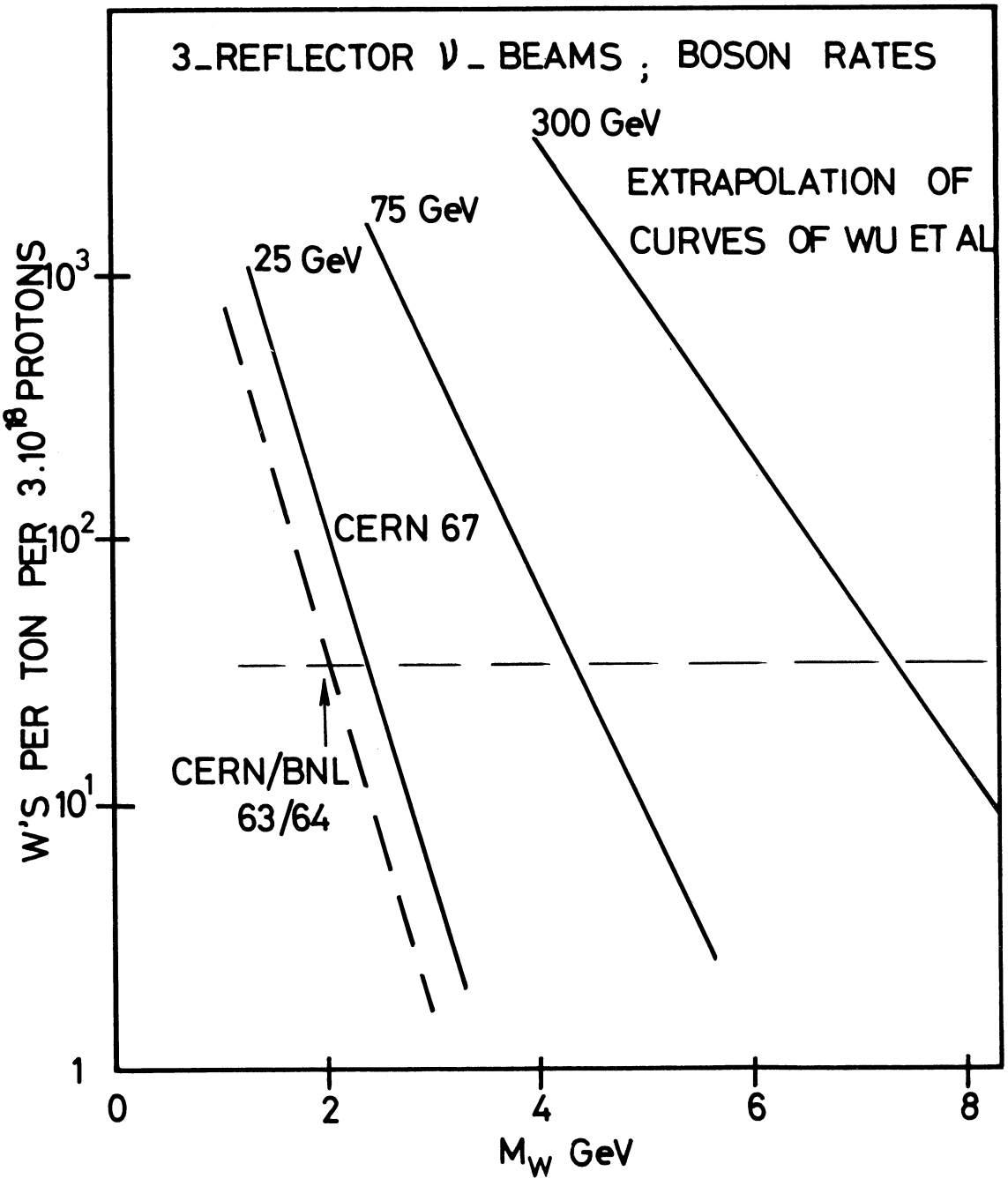

Fig. 2. Estimated Boson production rates, as a function of mass, for three different proton beam energies. The shielding, target and focussing systems were scaled up versions of the existing CERN 3-element system (See report by W. Venus, CERN Neutrino Conference, Jan. 1969). The curves are based on extrapolation of the calculations of Wu et al[4]. The horizontal dotted line refers to the level of the CERN/BNL experiments (1963/64).

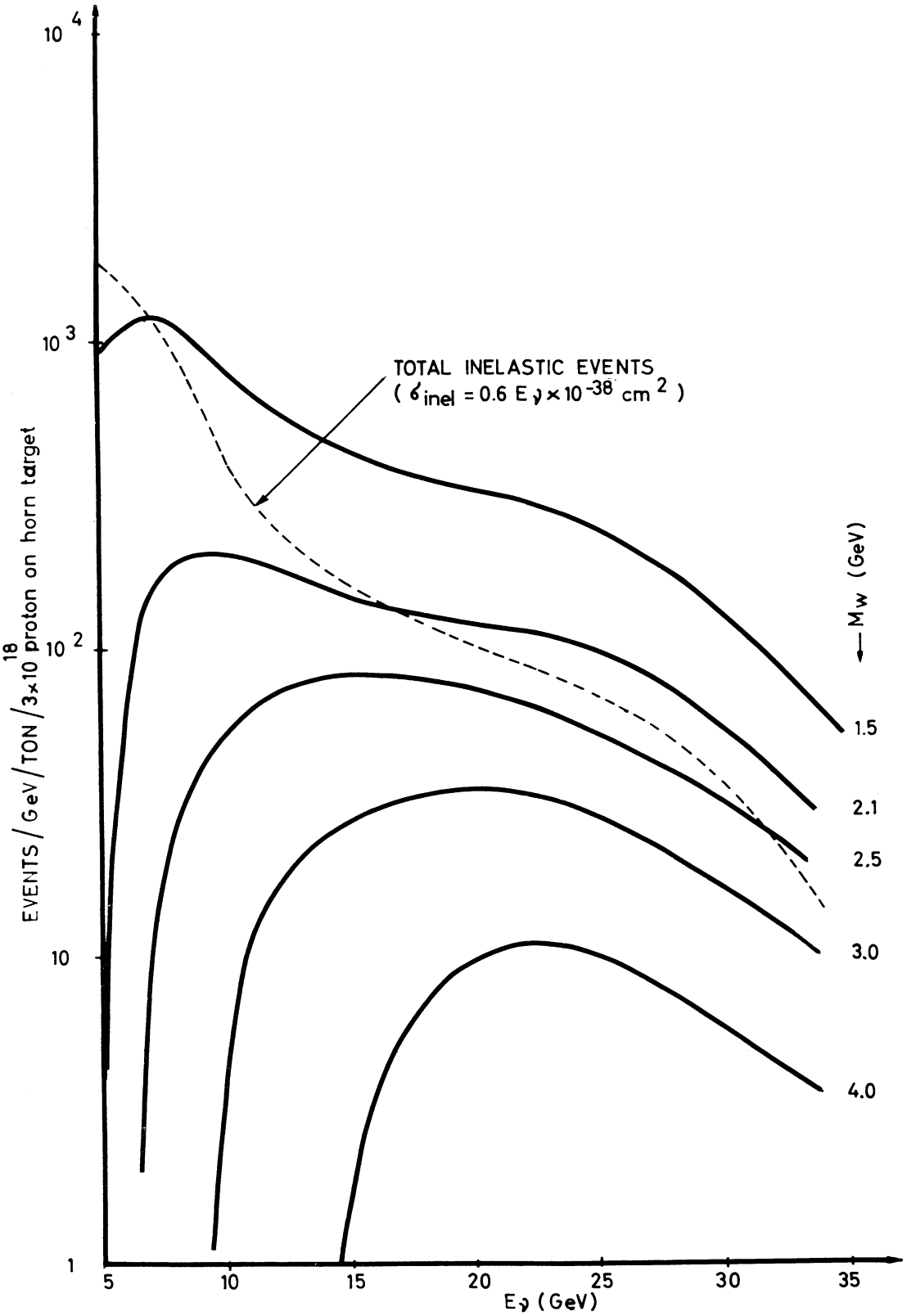

Fig. 3. Differential boson production rates estimated for a neutrino installation at Serpukhov (75 GeV). For comparison, the total inelastic rate, based on the data of Fig. 23 extrapolated to higher energies, is shown by the dotted curve.

particles. I mention here only one such recipe, or class of recipes, since it clearly differentiates two types of weak process. Gell-Mann et al [7] divide the current - current interactions into diagonal terms (D) - consisting of a weak current such as (νe, e) interacting with itself - and the rest, or non-diagonal (ND) terms. The ND processes, such as μ-decay, are then given by the first-order Fermi term, since all ND higher order terms are small ($\sim G^{2n}$) and any higher-order D terms are either finite and small, or can be made so with a cut-off. All the unpleasant singularities are dumped instead into the D interactions, about which nothing firm can be said, but whose couplings might be very large.

There are only two obvious diagonal interactions which could be studied with neutrino beams. They are νe - e elastic scattering and μ-pair production by ν_μ in a Coulomb field - see Fig. 4. According to the Fermi theory, process (i) has a cross section

$$\sigma_1 = \frac{G^2}{\pi} (2m_e E_\nu) = \frac{1.5}{10^{41}} E_\nu \quad \text{cm}^2/\text{electron}$$

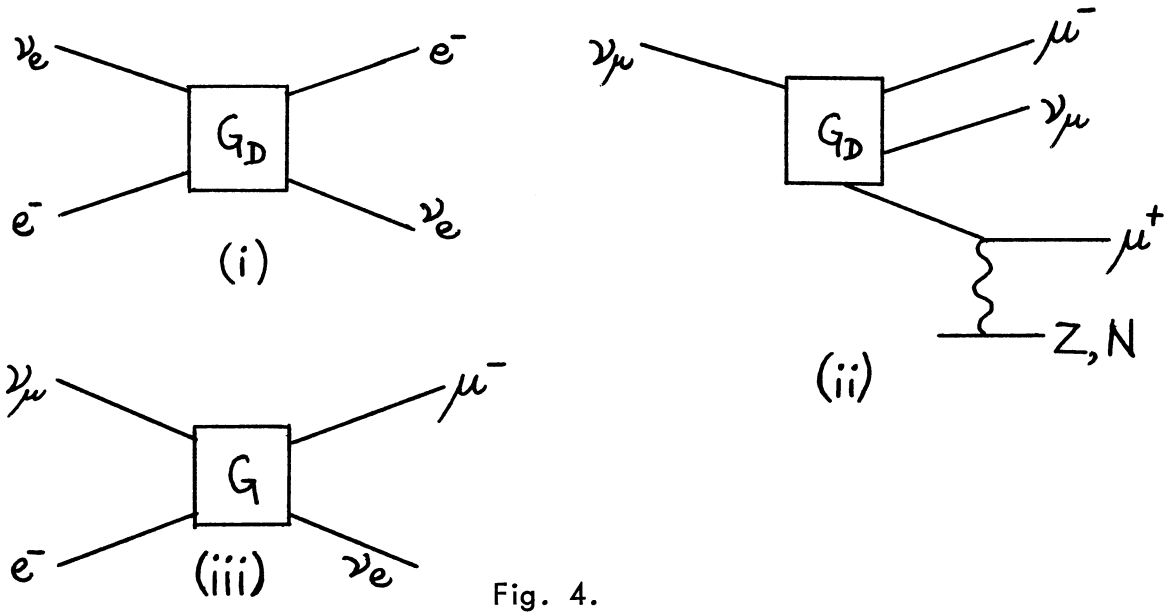

Fig. 4.

Process (ii) has been computed by Czyz et al [8] on the basis of the Fermi interaction. Summing both incoherent and coherent contributions - the latter

dominating for $E_\nu >$ a few GeV - they obtain for example

$$\sigma_2 = 2.7.10^{-41} \text{ cm}^2/\text{Fe nucleus for } E_\nu = 10 \text{ GeV}$$

$$= 1.6.10^{-40} \quad " \quad " \quad " \quad = 30 \text{ GeV}$$

$$= 9.10^{-40} \quad " \quad " \quad " \quad = 100 \text{ GeV}$$

Above 100 GeV one is in the asymptotic region, where σ varies as $E_\nu . \ln (E_\nu / m_\mu)$.

Fig. 5. gives event rates for these reactions for the CERN 25 GeV beam. The units of detector mass are 100 tons, and of integrated proton flux 3.10^{18} protons on the target - these numbers representing roughly the total mass and flux in all accelerator neutrino experiments to date. For comparison, the rate for the ND process (iii) of inverse μ-decay ($\nu_\mu + e^- \rightarrow \mu^- + \nu_e$) is included. The cross-section is

$$\sigma_3 \simeq \frac{G^2}{\pi} \frac{(2m_e E_\nu - m_\mu^2)^2}{2m_e E_\nu}$$

with a threshold $E_\nu = m_\mu^2 / 2m_e \sim 11$ GeV.

The rates for all three processes, based on conventional weak coupling, are dismally low. For a 200 - 400 GeV accelerator, one would expect, for the units of Fig. 5., a total of ~ 50 (νe, e^-) scatters, ~ 100 cases of the μ - pair process, and roughly 500 (ν_μ, e^-) scatters. As far as event rates are concerned, it might therefore be just possible to obtain a quantitive comparison of the diagonal and non-diagonal couplings, G_D and G. However, the experimental problems of recognizing, in large spark chambers, such events against the background inelastic processes on nucleons, at least 3 orders of magnitude more intense, are nightmarish.

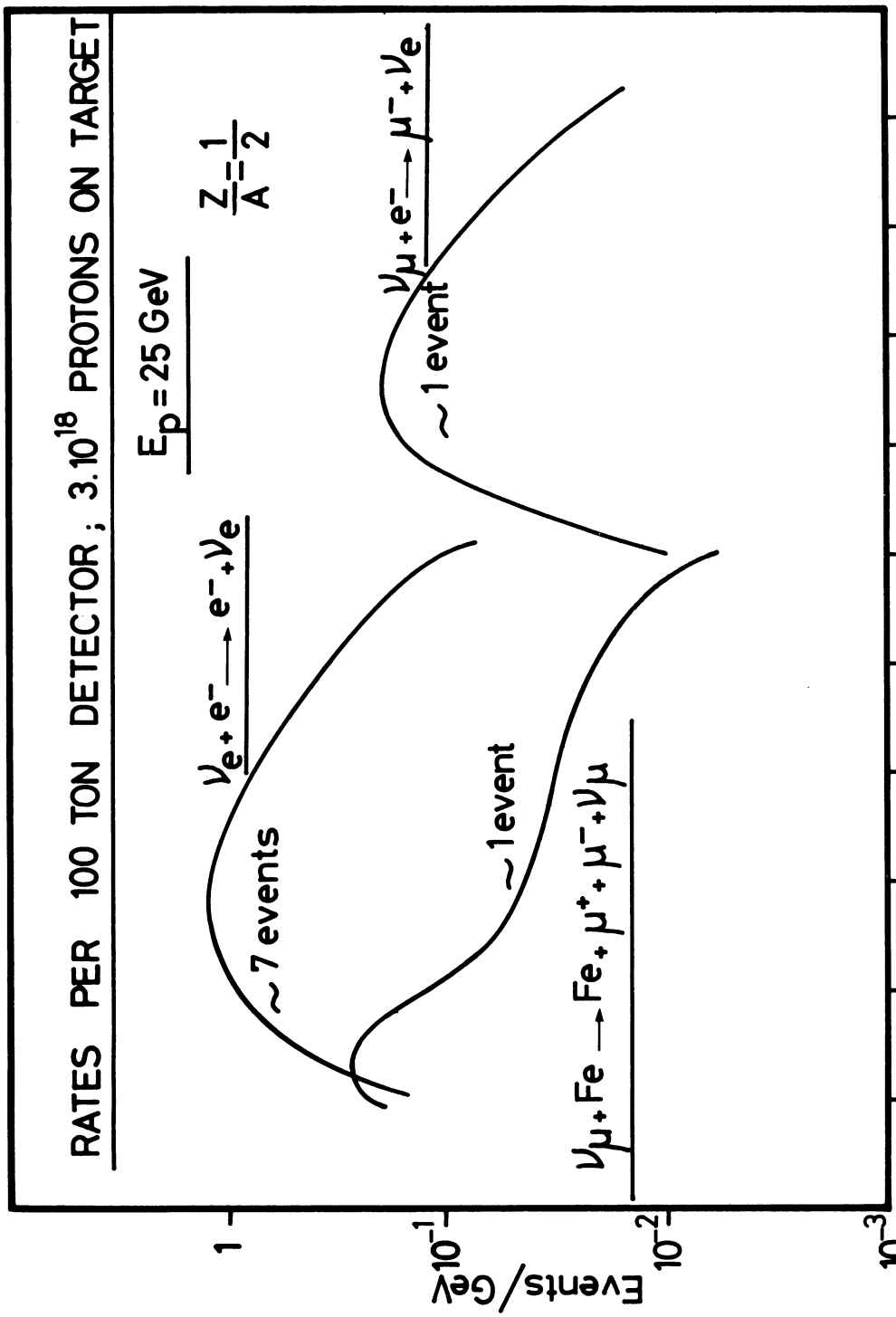

Fig. 5. Rates for 3 purely leptonic processes calculated for the CERN (25 GeV) neutrino beam.

Of course, the situation may be much better, if $G_D^2 \gg G^2$. An upper limit to G_D can be set from existing experiments. In the CERN bubble chamber experiments, the product (total number of protons x detector mass in tons) was $\sim 4.10^{17}$, or $1.3.10^{-3}$ of the units of Fig. 5. A (νe, e) scatter yielding a single high-energy ($\sim$ 5GeV) electron within an angle $\sim \sqrt{2m_e/E_\nu}$ $\simeq 1^\circ$ of the ν -beam direction, would have been easily recognized; none was seen. This allows one to set the limit

$$G_D \lesssim 10\, G_{Fermi}$$

1.4 Neutral currents

The limits which one can place on the coupling of neutral currents in neutrino experiments are essentially set by neutron background. The best values are given by exploiting the free proton kinematics in the CERN propane experiment:-

a) $\sigma\ (\nu + p \rightarrow \nu + p) < 0.5\ \sigma_{elastic}$,

b) $\dfrac{\sigma\ (\nu + p \rightarrow \pi^+ n\, \nu)}{\sigma\ (\nu + p \rightarrow \pi^+ p\, \mu^-)} < 0.08$

In the forthcoming hydrogen chamber experiments at BNL and ANL, these limits will be improved by at least a factor 5, since the carbon background will be absent. In the more distant future, further improvements would be possible with narrow band neutrino beams.

1.5 Other processes

Fig. 6. shows some unpublished work of Yoshiki,[9] of the CERN heavy liquid chamber group. What is plotted is simply the invariant muon-proton

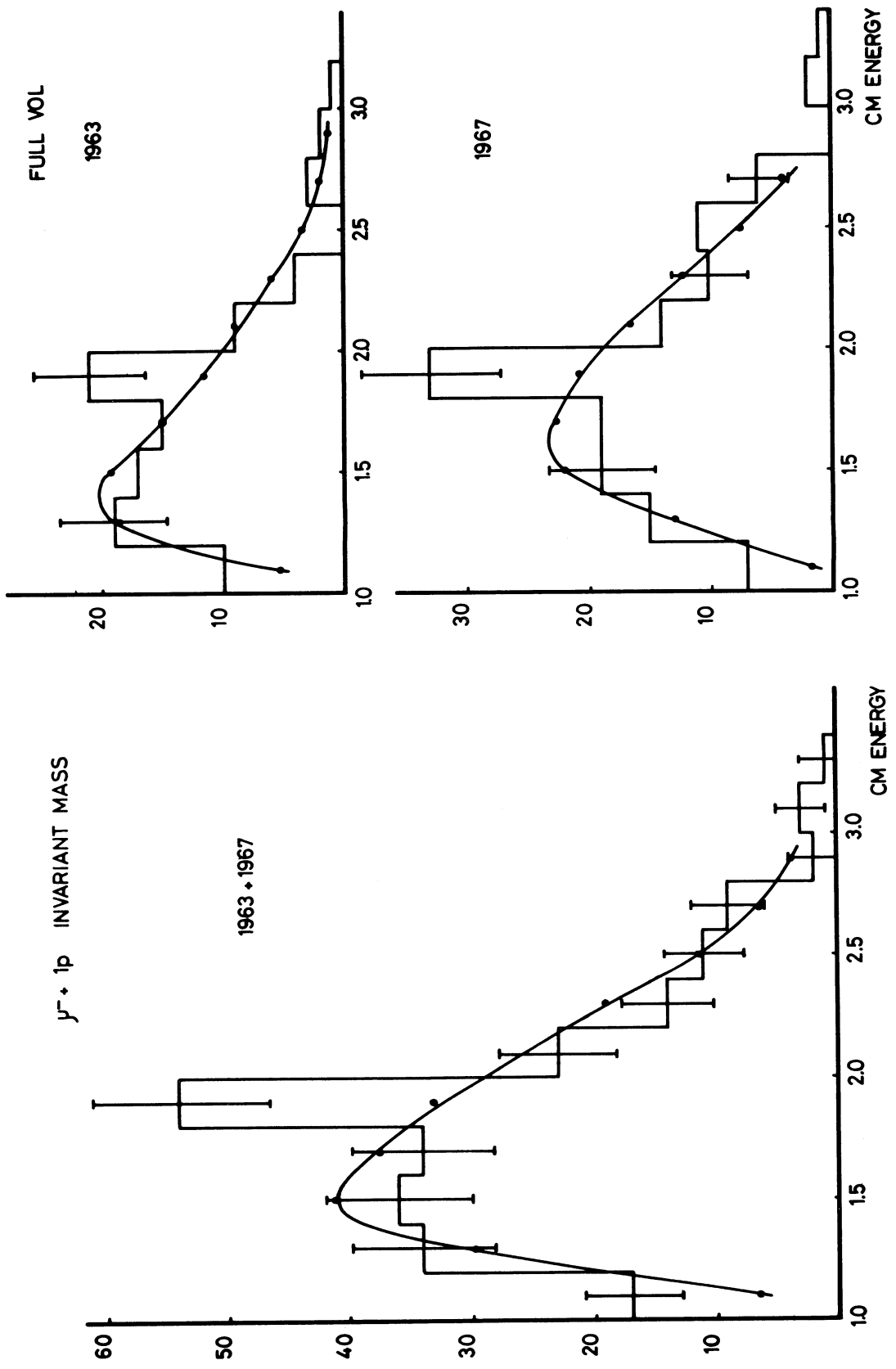

Fig. 6. Data on the invariant mass distribution of μ^- and proton in single proton events, in freon (1963), propane (1967) and for the combined data (left). The curves are the result of Monte-Carlo calculations based on the normal elastic process $\nu + n \rightarrow \mu^- + p$.

mass, for events containing a negative muon and a single proton. We expect these to be examples of the usual elastic process, $\nu\mu + n \rightarrow \mu^- + p$. The curves are from Monte-Carlo calculations, using as imput the neutrino spectrum, standard form factors ($M_A = M_V = 0.84$ GeV) and a Fermi - gas nuclear model. There is an excess of events in the 1.8 - 2.0 GeV bin, correspondi ng to a neutrino energy of 1.3 GeV in both the 1963 (freon) and 1967 (propane) data. The total effect is some 2.8 standard deviations. It is very likely just a statistical effect. If it is a real physical effect, it might be accounted for in terms of an S-channel resonance, carrying the rather odd quantum numbers J = 1, B = L = 1 (Fig. 7.)

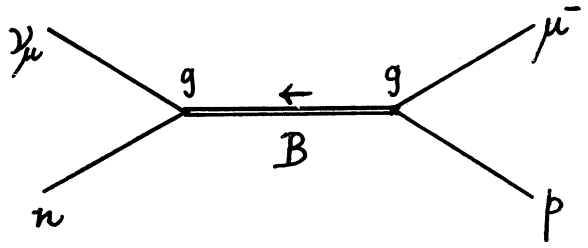

Fig. 7.

A scalar particle is excluded, from the muon angular distribution. A vector particle B would be polarized as shown and would decay emitting the muon in the forward direction, from helicity considerations. The muon angular distribution in the centre-of-mass cannot contain terms higher than $\cos^2\theta$. The most general form of the distribution contains 3 unknown parameters; the simplest possibility is to set two of these zero, yielding a $(1 + \cos\theta)^2$ variation. Unfortunately, the muon angular distribution from the normal elastic process is even more strongly peaked forward, and swamps that from the possible B - decay. From the observed rate one obtains

$$\pi \lambda\!\!\!^{-2} \cdot \Gamma_{true} = (\sigma_{average})_{observed} (\Gamma)_{observed}$$

where the apparent width is contributed by experimental errors. This relation gives $\Gamma_{true} \sim 10^{-3}$ eV, or a lifetime $\tau \sim 10^{-12}$ secs. Thus the object B will escape the parent nucleus before decaying - otherwise one would not observe a well-defined peak in the mass spectrum. From Γ_{true} one can deduce that the effective coupling g, is of order 10^{-3} of the Fermi coupling.

Evidence confirming or rejecting these interesting results should shortly be obtained in experiments with large hydrogen chambers, at ANL and BNL. Their approximately fourfold better momentum resolution should be quite decisive.

2. SEMILEPTONIC INTERACTIONS

2.1 The Elastic Process $\nu + n \rightarrow \mu^- + p$.

There have been a number of experiments attempting to measure the form-factors in the elastic process, and the results are displayed in Table 1. The last two entries are new results not previously reported.

The theoretical assumptions made in the analysis are perhaps worth stating. Assuming the V-A interaction and G - and T-invariance, and supposing the boson mass to be very large, the matrix element will contain 2 vector and 2 axial vector form factors. One of the axial terms (the so-called induced pseudoscalar term) is very small and is neglected. Assuming CVC, the 2 vector terms are equated to the isovector electric and magnetic form-factors, respectively, leaving one axial form-factor to determine. This is parametrized by the dipole formula

$$\frac{G_A(q^2)}{G_A(O)} = \frac{1}{\left(1 + \frac{q^2}{M_A^2}\right)^2}$$

in analogy with the formula for the vector form factor (where $M_V = 0.84$ GeV) Thus, the experiments seek to determine one number, M_A.

In all the experiments, the reactions occur in complex nuclei. One must then take account of (i) the Pauli principle and the Fermi motion of the target neutron (ii) scattering and/or absorption of the proton in traversing the nucleus , (iii) background contributed by events of the type $\nu + N \rightarrow N' + \pi + \mu^-$, in which the pion is absorbed by the nucleus.

The approach to these problems in the early CERN freon chamber experiment was as follows.[10] Monte-Carlo calculations demonstrated that genuine elastic reactions would appear almost exclusively as events with single protons > 30 MeV, whereas those containing absorbed pions would appear almost exclusively as multiproton events. So, the procedure was simply to assume that all non-pionic events with a single proton were elastic candidates. The neutrino energy was equated to the visible energy E_{vis}, since calculations showed that, although the product proton might be severely scattered, it would not lose much energy in escaping the nucleus; in any case, if one selected events of $E_\nu > 1$ GeV, the bulk of E_ν is accounted for in the energy of the charged lepton. Since the neutrino direction, as well as the muon direction, is well known, one can determine q^2 with small error. One can also deduce the effective recoiling hadron mass, M*, from

$$q^2 = M^2 - M^{*2} + 2M(E_\nu - E_\mu)$$

where M is the mass of the target nucleon, assumed stationary. Then, allowing for Fermi motion, the values of M* obtained peaked symmetrically around M, showing that the inelastic contamination was small. The method of finding

M_A was to fit the shape of the q^2 - distribution - allowance being made for Pauli principle and Fermi motion - for events of $E_\nu > 1$ GeV, in order to reduce dependence on the neutrino spectrum shape.

Lovseth[11] has shown that the systematic uncertainties in the result, as judged by repeating the calculations for extreme nuclear models, is of order of the statistical error.

The second and third result of Table 1, come from spark chamber experiments In the CERN experiment [12] - see Fig. 8 - the estimated inelastic contamination was ~ 45%; an attempt was made to subtract this using the theory of N* (1238) production by Berman and Veltman [13], but this involves assumptions about the inelastic form-factors. A similar criticism can be made of the ANL experiment of Kustom et al [14]. Making the selection $p_\mu > 0.3$ GeV/c, they expected to reduce the inelastic background to ~ 10%. However, their q^2 distribution (Fig. 9) does not show the expected decrease at small q^2 due to the Pauli principle. If all the excess is attributed to inelastic background, the latter will be of order 25%.

The final result in Table 1 comes from the CERN propane [15] chamber experiment, where the elastic events occur in carbon, and the improved momentum resolution, as compared with heavy freon (roughly a factor 2) leads to better constraints in selection. Fig. 10 shows the scatter plot of q^2 versus M^{*2}, for events of $E_\nu > 1$ GeV with single identified protons, as well as events (C-events) with a single positive secondary ambiguous between pion and proton ($p > 750$ MeV/c). δ-ray counts established that, statistically, 87% of the ambiguous secondaries were in fact protons. The dotted curves in Fig. 10 indicate the expected spread in M* as a function of q^2, arising from Fermi motion. Some 25% of events lie outside the expected limits. Thus,

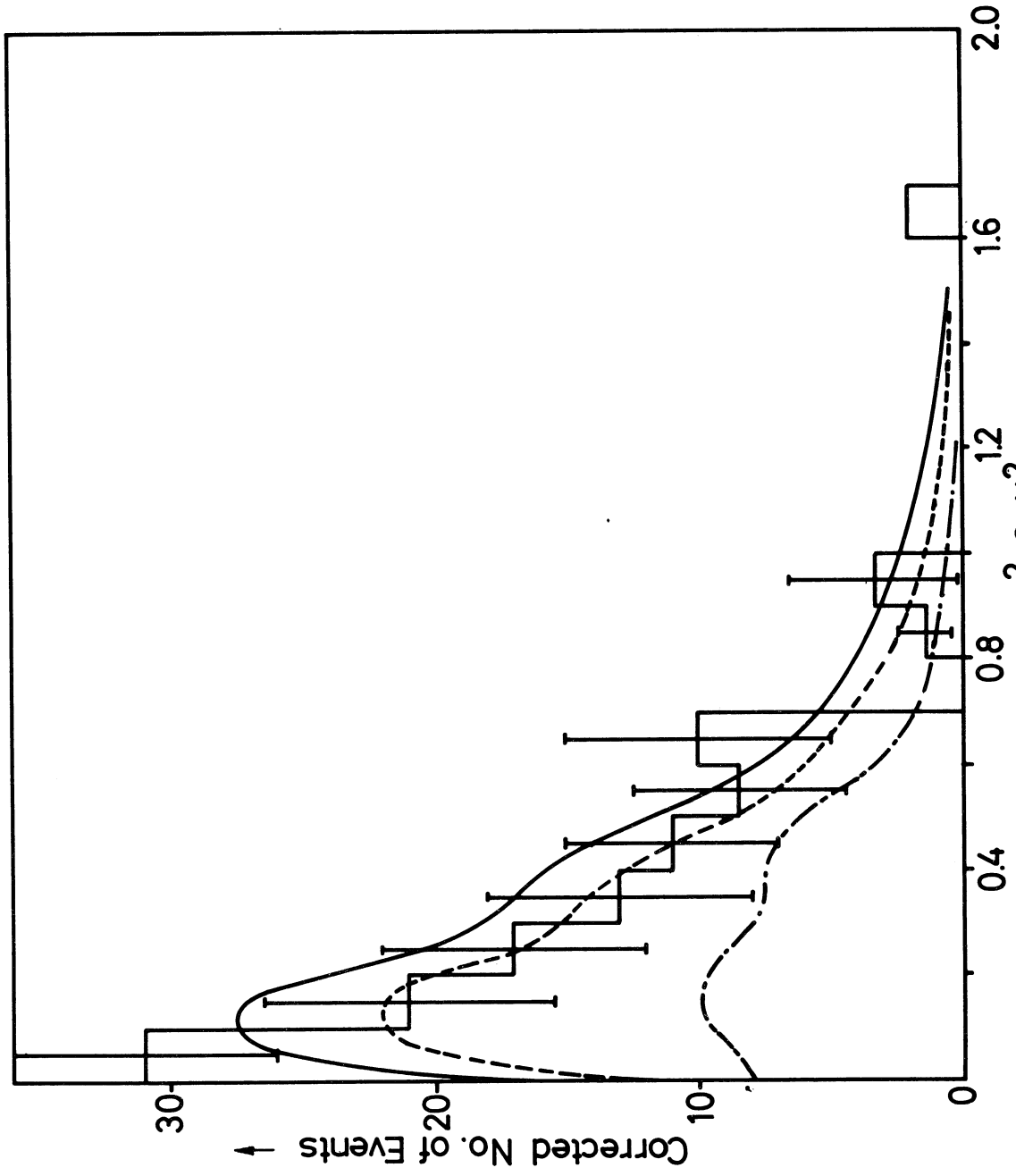

Fig. 8. q^2 distribution of elastic candidates observed in the CERN SC experiment (Al)[12) - inelastic + elastic (M_A = 0.84 GeV); --- inelastic + elastic (M_A = 0.5 GeV); -.-.-. inelastic contamination.

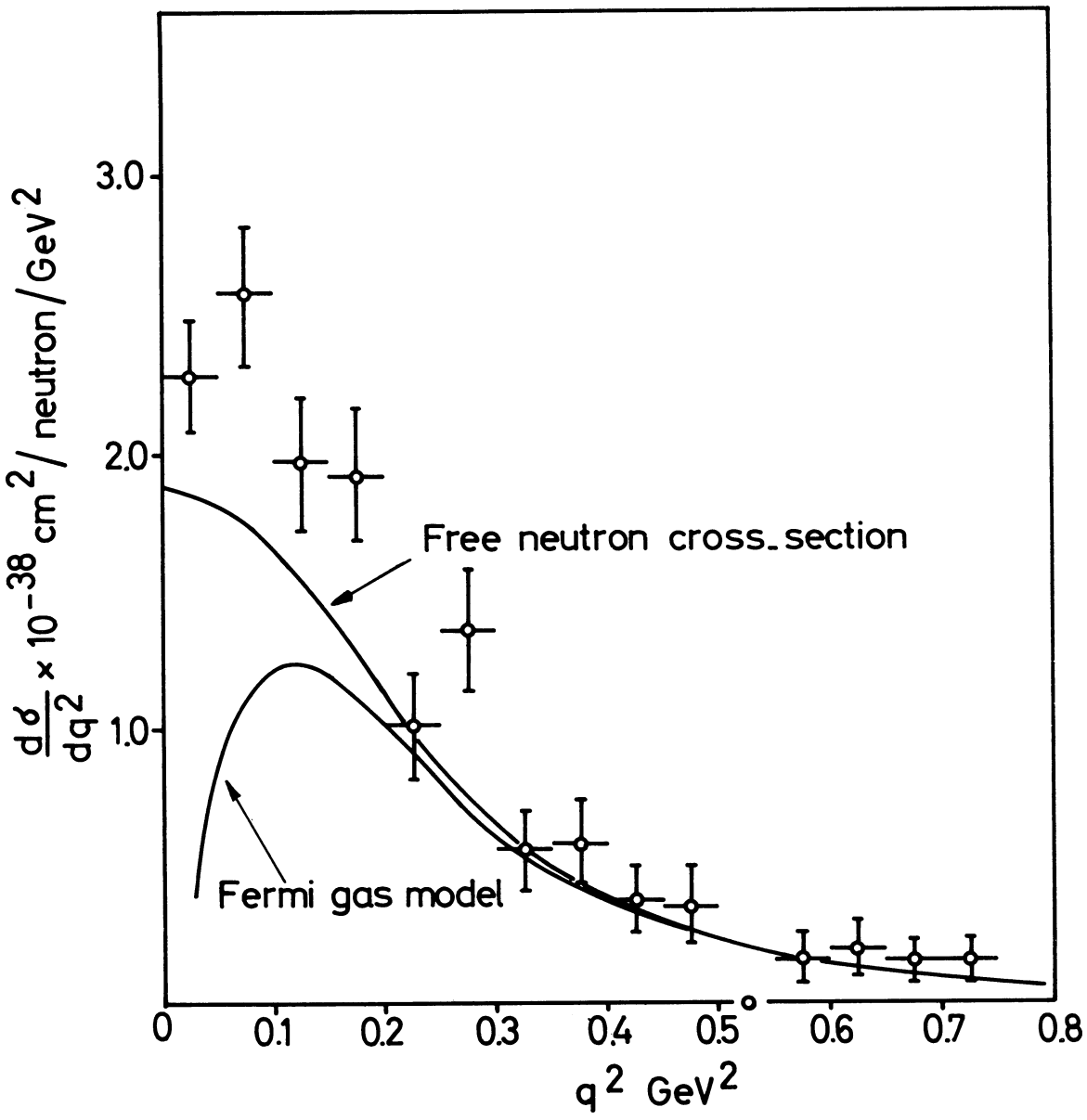

Fig. 9. q^2 distribution of elastic candidates observed in the ANL SC experiment (Fe)[14]. The curves are the distributions expected for the elastic process, and for M_A = 1 GeV.

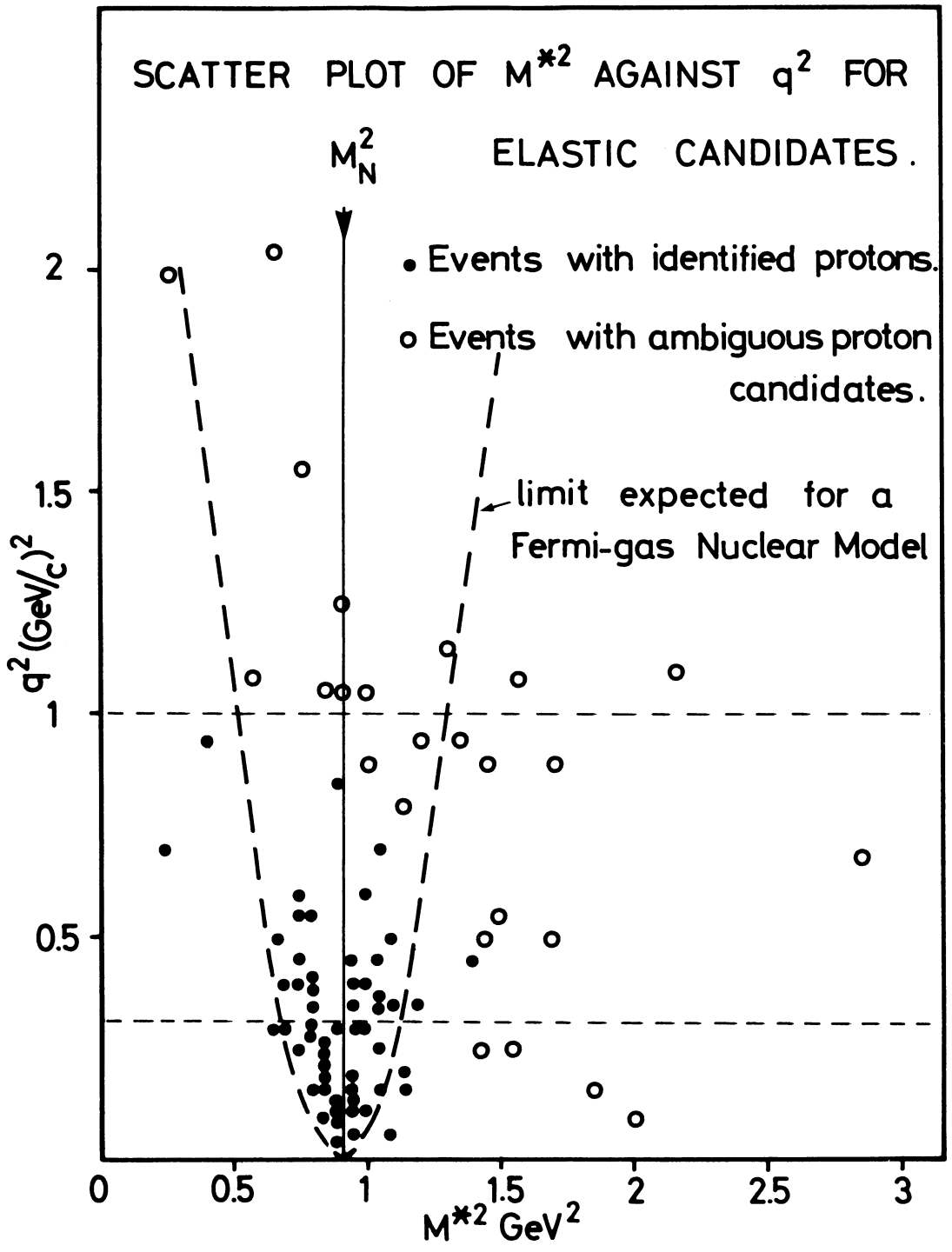

Fig.10. CERN propane bubble chamber data [15] on elastic (single proton) candidates. •- identified protons; o - ambiguous π^+/p events (87% are protons).

Table 1

Experiment	Method	Nuclear model dependence	N* background	Quoted flux error	M_A, GeV
CERN CF_3Br BC[10]	q^2-shape	Yes	~10%	$\pm$ 30%	0.75 ± 0.25
CERN Al SC[12]	q^2-shape	Yes	~45%	$\pm$ 30%	0.65 ± 0.42
ANL Fe SC[14]	q^2-shape	Yes	10-25%	----	1.05 ± 0.2
CERN C_3H_8 BC	ν-flux	No	10%	$\pm$ 15%	0.73 ± 0.2

the inelastic background inside the limits may be considerable, even though the distribution is symmetric about the nucleon mass. Events inside the Fermi limits and of $q^2 < 0.3$ GeV^2 were also excluded in order to make the analysis independent of the nuclear model, as also were those of $q^2 > 1$ GeV^2 in order to reduce dependence on ν - spectrum shape and to reduce inelastic background. The ν-flux in this experiment had been well determined in separate runs, by accurately measuring the muon distributions inside the shield. The absolute number of elastic candidates, inside the Fermi boundary and of $1 > q^2 > 0.3$ GeV^2 could then be used to compute M_A. Other selection criteria gave similar results. A plot of $\sigma_{elastic}$ v. neutrino energy is given in Fig. 11 for comparison with various M_A values.

The discussion above illustrates some of the problems encountered in attempting to determine M_A from events in complex nuclei. It is clear that the values of M_A quoted are subject to severe systematic errors, and all that the results prove is that M_A and M_V are about the same. With the forthcoming deuterium experiments, at ANL and BNL, some, but not all, systematic errors will be removed. The results will always be at the mercy of errors in knowledge of the ν-flux and spectrum shape. Let us also remember that M_V is itself known only to $\pm$ 5%. One can hope that, with very careful analysis,

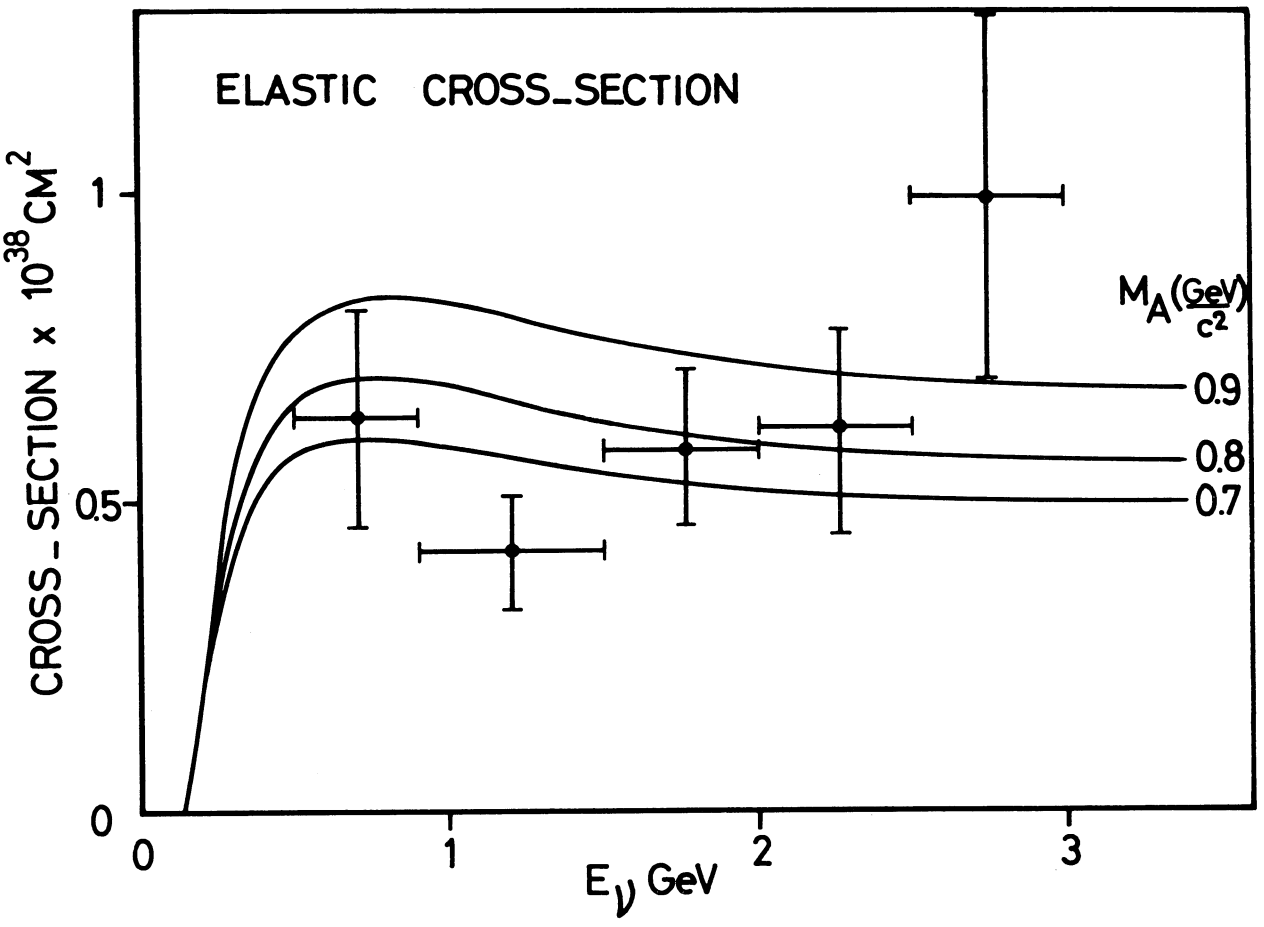

Fig. 11 Elastic cross-section versus neutrino energy, deduced from the CERN propane data.

the deuterium experiment might approach an absolute accuracy of order 10% in M_A - always assuming CVC to hold good.

2.2 Weak Pion Production

The propane chamber experiment at CERN has made it possible to obtain examples of the reaction

$$\nu + p \rightarrow p + \pi^+ + \mu^-$$

on free protons, with relatively small carbon background.[16] This reaction has the nice feature that it is kinematically well determined, and proceeds through a single ($I = 3/2$) isospin channel. If we define the x-axis along the neutrino beam, a selection of candidates for the above reaction was made by requiring $\Sigma p_x > 0.3$ GeV/c, in order to remove contamination of incoming π^+ masquerading as outgoing μ^-. Fig. 12 shows a scatter plot of $(p_x)_{unbalance} = E_{vis} - \Sigma p_x$ - a quantity which should be zero for a massless neutrino hitting a stationary proton - versus p_T, the resultant momentum component transverse to the neutrino beam. The free proton events cluster around the origin, with a spread accountable from measurement errors. Free proton events are defined as those for which $(p_x)_{unbalance} < 0.12$, $p_T < 0.24$ GeV. The carbon background among these 49 events has been estimated by comparing with $\mu^- p$ elastic events in the carbon (Fig. 13.), and also $\mu^- \pi^+ p$ events in freon (Fig. 14.) - in both of which the smearing due to Fermi motion should be similar. Comparing Figs. 12, 13, and 14 it is concluded that the free proton candidates contain $15 \pm 5\%$ carbon background. Other background corrections, e.g. $n \rightarrow \pi^- p \pi^+$, $\pi^+ + \text{nucleus} \rightarrow \text{nucleus} + \pi^+ + p$, $\nu + p \rightarrow n + \mu^- + \pi^+ + \pi^+$ (ambiguous), are negligible in comparison.

Fig. 15 shows the distribution of M*, peaking around the N* (1238) resonance, as expected. Fig. 16. displays the distribution of the Berman-Veltman angles[13]. On the left is the distribution, in the N* frame, of the polar angle θ between the π^+ and the bisector of the angle α between the neutrino and muon directions. For α small, it should have the form $(1 + 3 \cos^2 \theta)$, as observed. The azimuthal distribution should however be flat, contrary to observation. It is also found that there is an up-down asymmetry

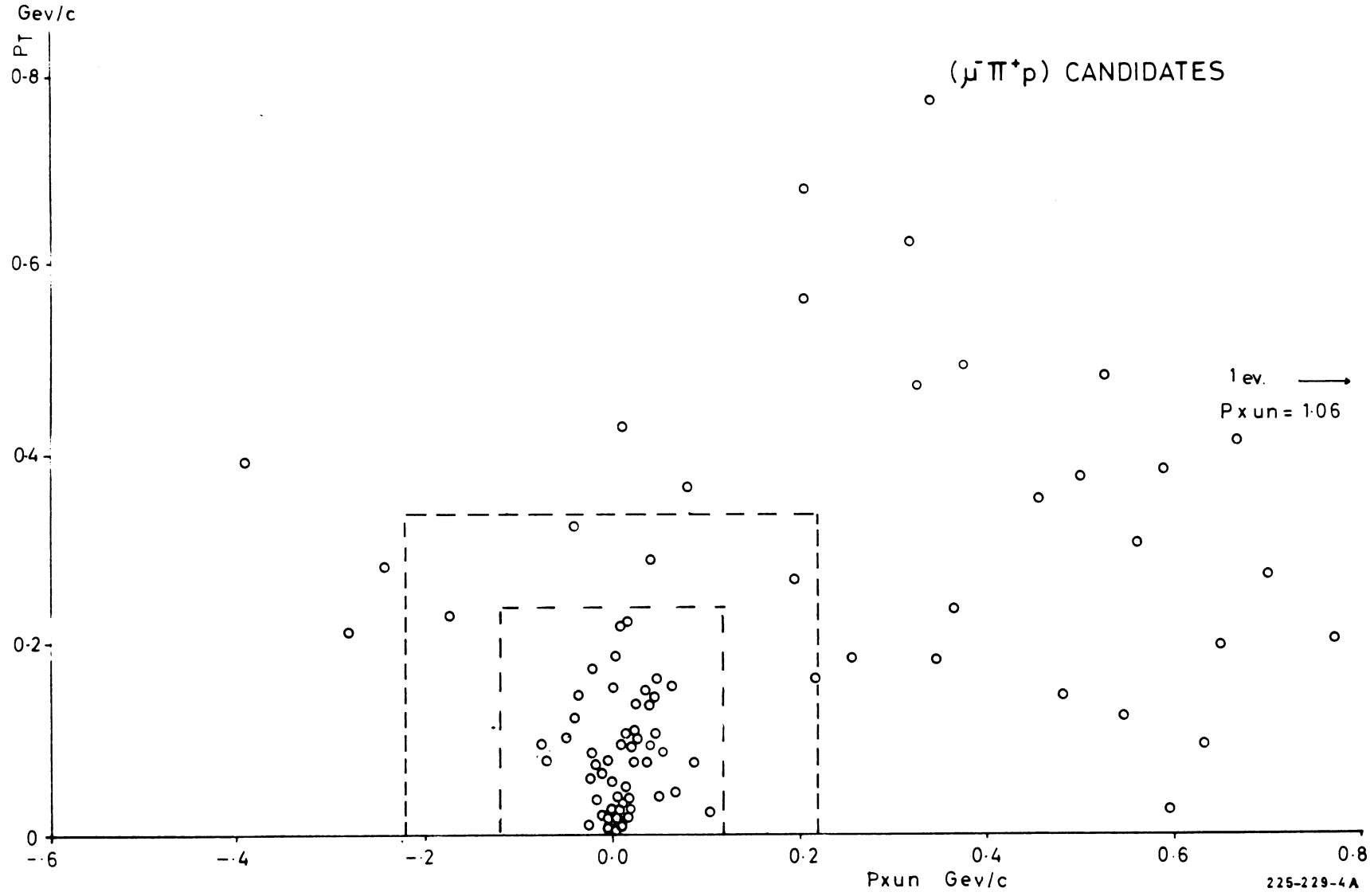

Fig.12. Distribution of $(p_x)_{unbalance} = E_{vis} - \Sigma p_x$ for $\mu^- \pi^+ p$ events in propane. The points lying within the inner box are ascribed to free protons. Events between the inner and outer box are used to obtain normalization of the carbon background (see Figs. 13 and 14).

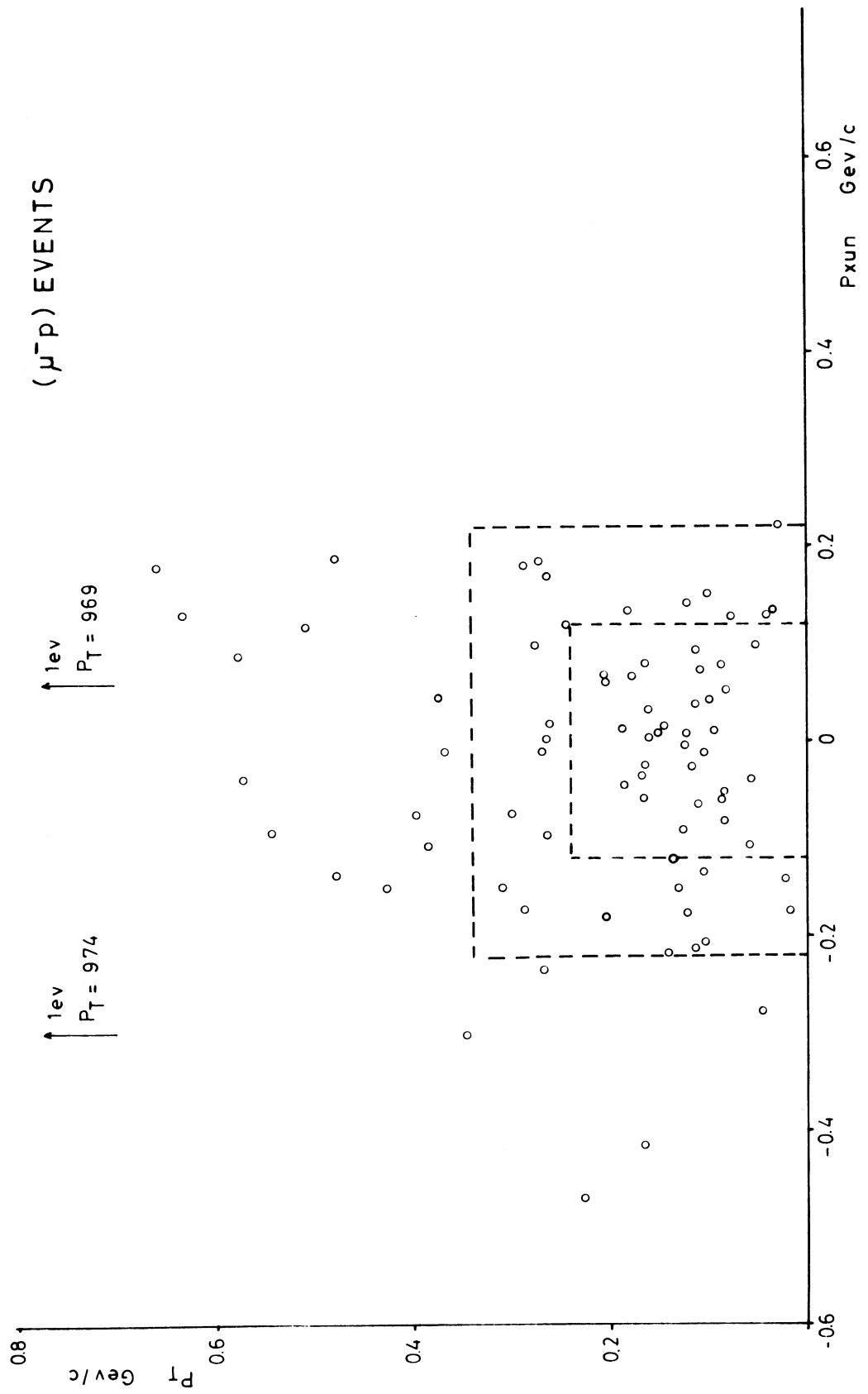

Fig.13. Same plot as Fig.12, for $\mu^- p$ events in propane. The carbon background in the "free proton events" of Fig. 12 is determined by comparing the ratios of numbers in the inner box, and between the inner and outer box, in either case.

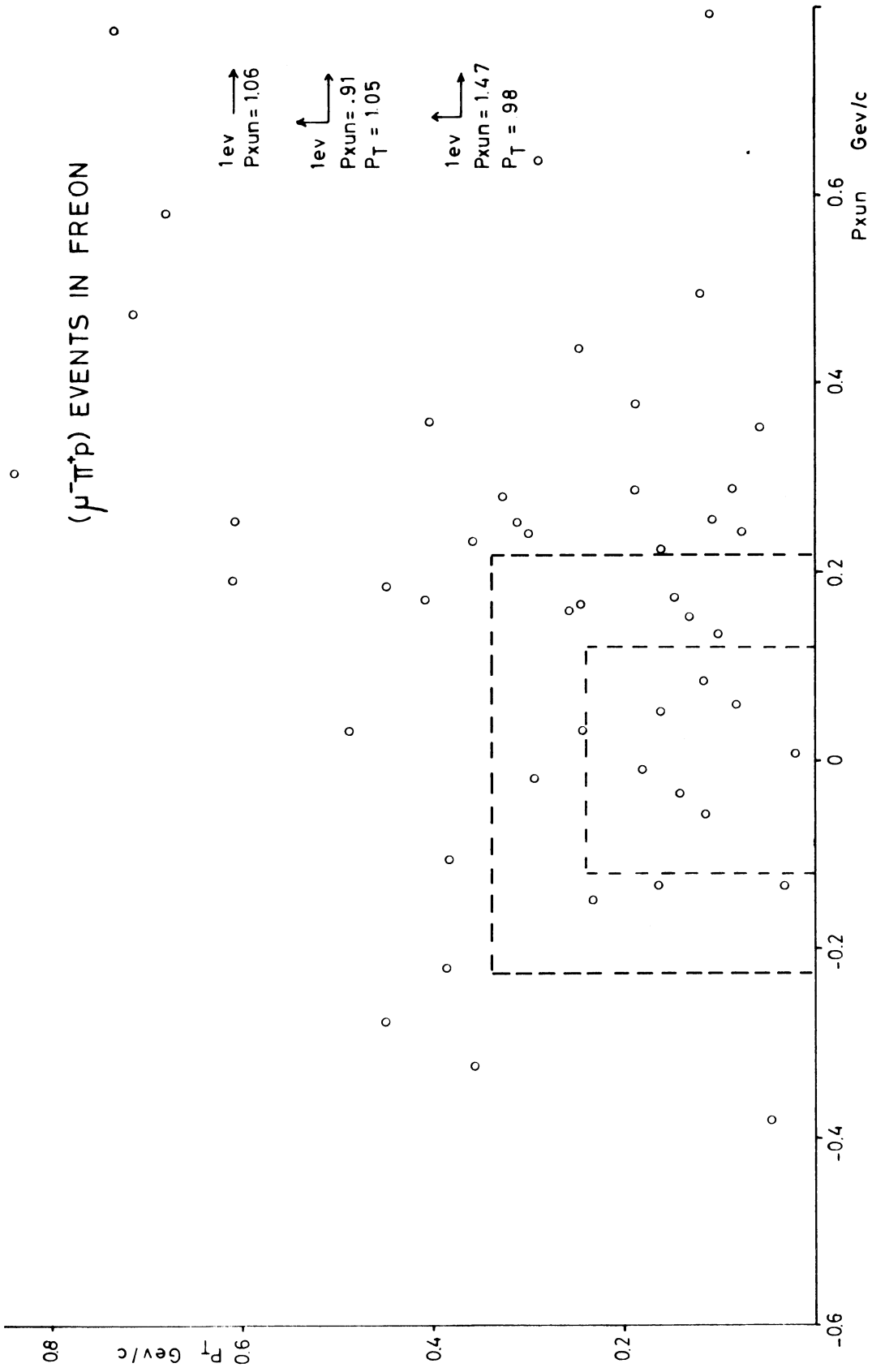

Fig.14. $\mu^-\pi^+p$ events in the freon chamber, allowing an independent determination of carbon background, with a similar result to that obtained in comparing Fig. 13 and 12.

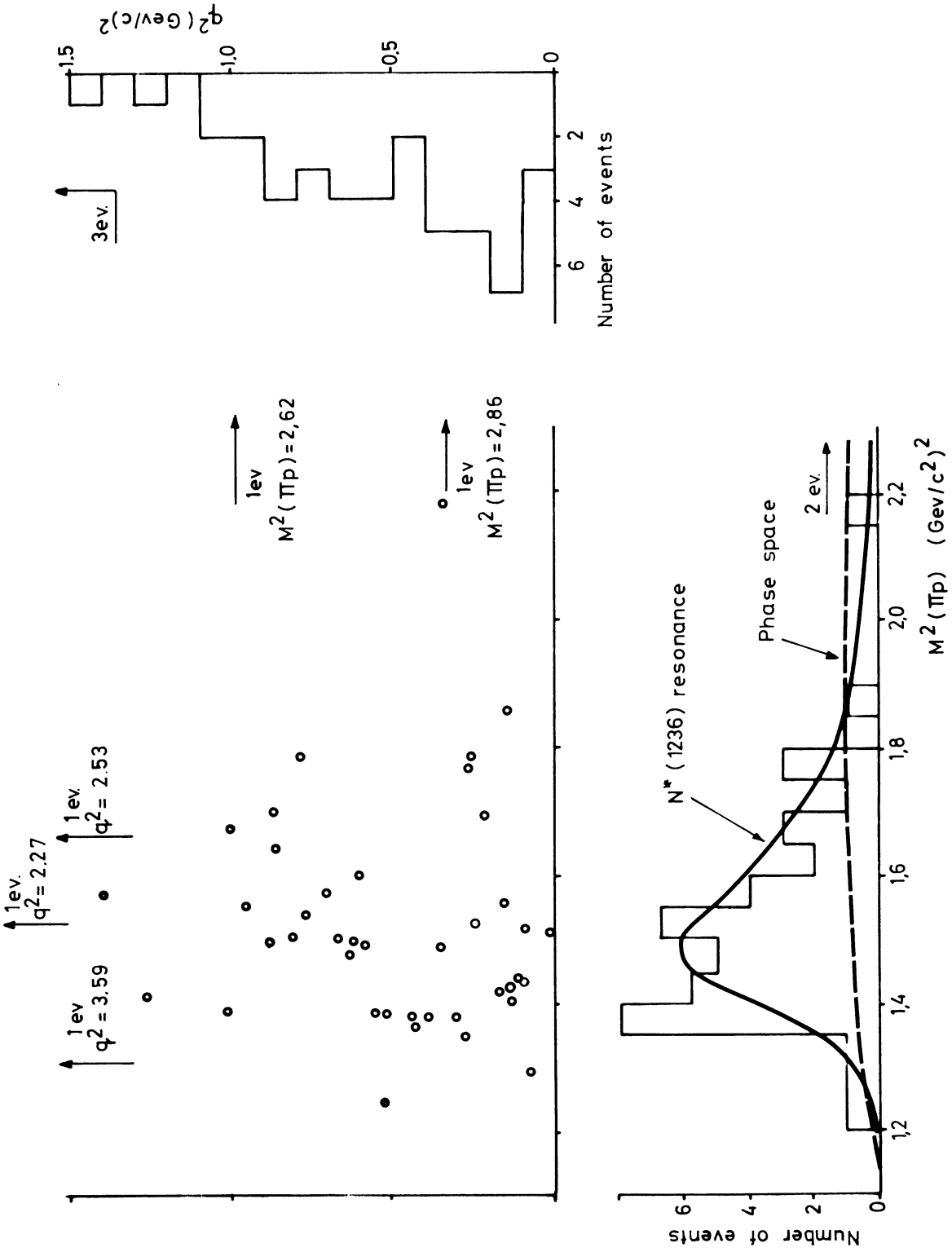

Fig.15. M* distribution of the free proton events of Fig. 12.

ANGULAR DISTRIBUTION OF π^+ IN (πP) REST FRAME

BERMAN VELTMAN ANGLES

'Hydrogen' Events, $\sin^2 \frac{\alpha}{2} < 0.1$, $1,3 < M^2(\pi P) < 1.9 \cdot (GeV/c^2)^2$

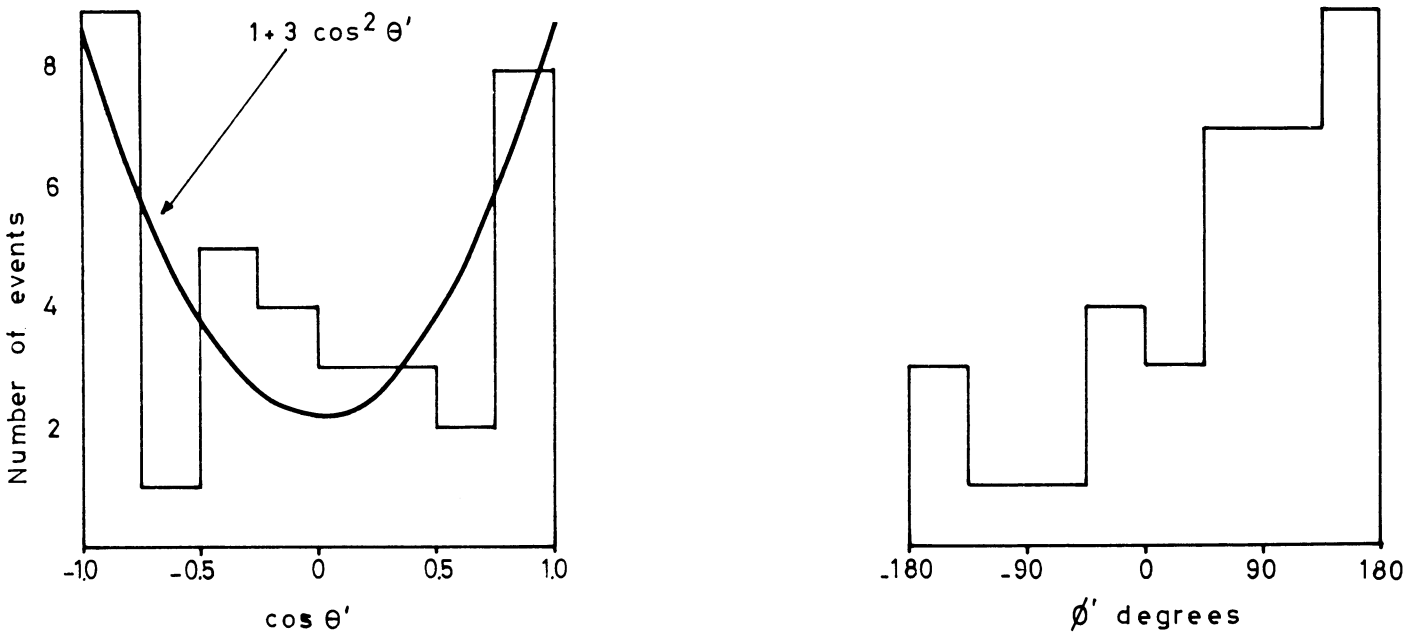

Fig. 16 The distribution of the Berman-Veltman angles in the free proton events The angles θ' and ϕ' refer to the direction relative to the bisector of the angle α between μ and ν, measured in N* rest-frame

of the π^+ with respect to the μ,ν plane. These facts suggest very strongly that, in addition to the dominant N* (3,3) resonant amplitude, there are strong interference terms from non-resonant contributions.

The observed cross-section on free protons is given in Fig. 17, as a function of neutrino energy, together with a sample of the numerous theoretical predictions. The main graphs which are expected to contribute are as follows:-

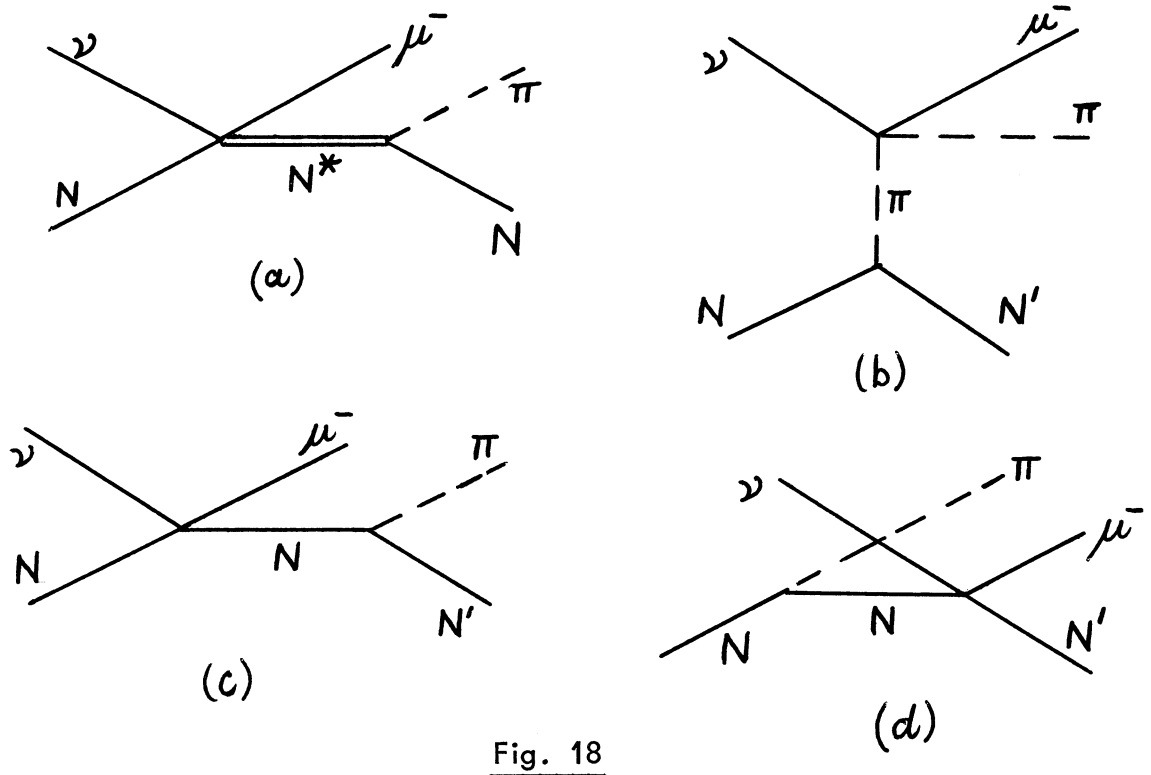

Fig. 18

The Berman-Veltman[13] calculation considered only the N* resonance term (a), obtaining the vector amplitudes from CVC and data on photoproduction, and the axial amplitudes from the Goldberger-Treiman relation and the static model. For both V and A terms, the appropriate form factors were taken equal to those for the elastic process (i.e. $M_A = M_V = 0.84$ GeV). In other calculations, for example those of Salin, the pion and nucleon - exchange

*) A full discussion of the theoretical models is given in a following paper by Franzinetti.

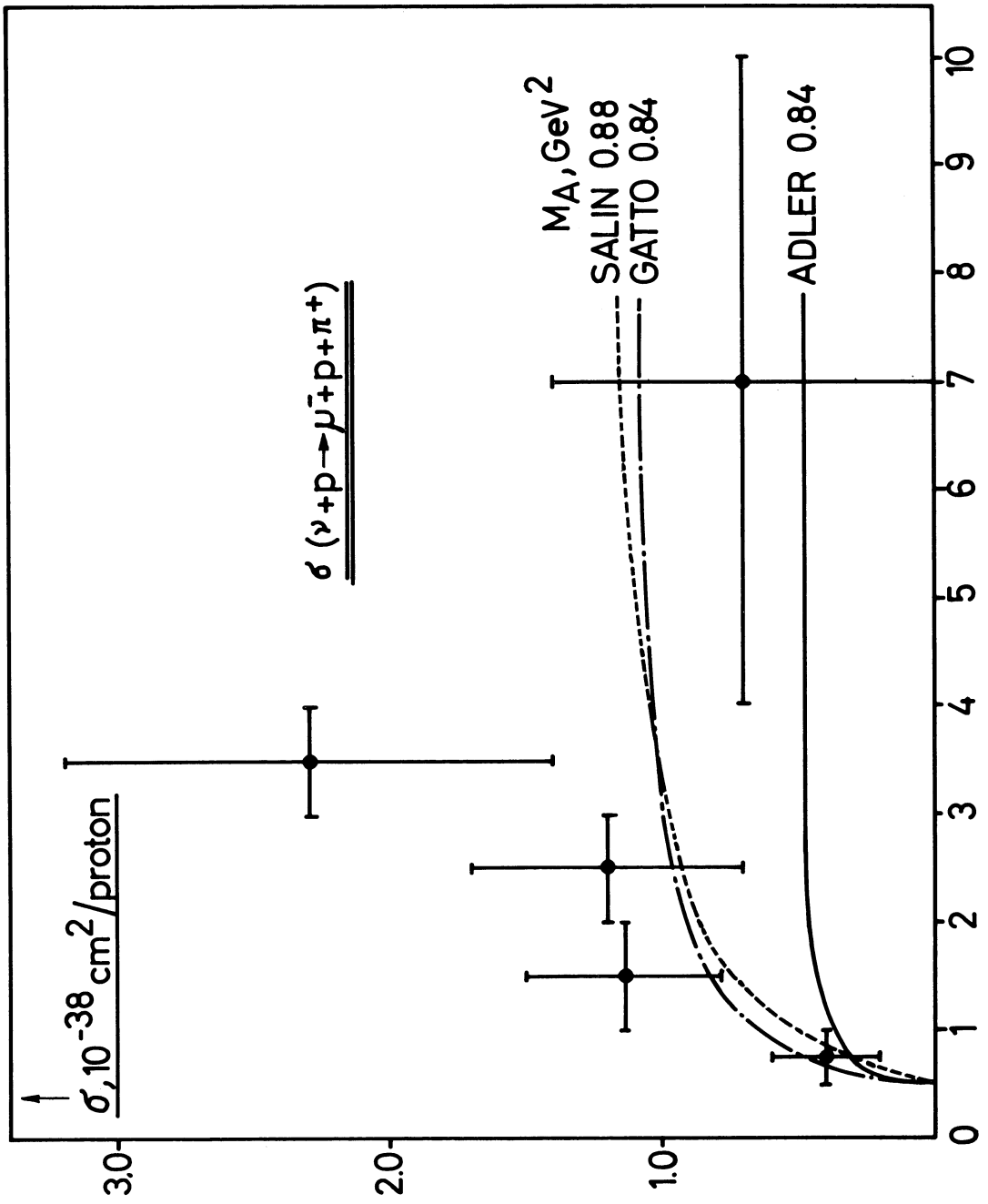

Fig.17. The cross-section for π^+ production on free protons, experimentally and according to a few theoretical models, for $M_A \sim 0.84$ GeV.

graphs (b), (c), (d) were included, though their effect on the cross-section is small.[17] Adler[18] has made a calculation assuming that all the amplitudes involved satisfy one-variable dispersion relations (at given q^2). His conclusions, namely that the vector contribution is dominated by the magnetic dipole term and the axial vector, by the electric dipole term, are similar to Salin's. Yet the cross-section computed by Adler is a factor 2 less than that of Salin.*

It is clear that the computation of cross-sections above is not a very sensitive test of the different theoretical models, and that a better understanding of the processes involved can only be obtained by detailed comparisons of angular distributions and charge ratios (π^+/π^o) as a function of M*. Much more experimental data is also needed, and this will be obtained in the near future in the large heavy-liquid and hydrogen chambers.

2.3 Adler Tests of PCAC

The famous Adler Theorem[19] concerns inelastic cross-sections for the so-called "parallel configuration", where the muon emerges exactly in the direction of the incident neutrino. If we neglect lepton mass, the leptons are then represented by null 4-vectors, proportional to one another. The only 4-vector which can enter the matrix element from the lepton vertex is then the 4- momentum transfer q_α (where $q_\alpha{}^2 = 0$). The product of this with the hadronic currents $J_\alpha{}^{V,A}$ is simply the divergence $\partial (J^V + J^A)/\partial x_\alpha$. From CVC, we expect the divergence of the vector current to be zero, and then from PCAC, the divergence of the axial current which remains, to be dominated by single-pion exchange. Thus, there should be a proportionality between the differential cross-section , $d\sigma/d\Omega$, for

$$\nu + N \rightarrow N^* + \mu^-, \qquad \theta_\mu = 0,$$

and the total cross-section for

$$\pi^+ + N \rightarrow N^*$$

for the same mass M* of the hadronic final state. The constant of proportionality contains known coupling constants, kinematic factors and lepton mass corrections[20]. Experimental verification of the Adler Theorem is bedevilled by the fact that, to extrapolate the cross-section to $q^2 = 0$ (where there are

no events), one must accept events over a finite range of θ_μ and q^2, where there will be also vector contributions. According to Adler, the latter should be very small (< 15%) for $\theta_\mu < 6^\circ$ (cos $\theta_\mu > 0.995$). Further, if everything is dominated by the one-pion pole, one should also have $q^2 < m_\pi^2$.

Fig. 19 indicates the data of Bonetti et al[22], in which the distribution of cos θ_μ is plotted for inelastic events in propane, for all values of q^2. The shaded area between the curves shows the predicted event rates according to the Adler Theorem; the uncertainty arises from (i) errors in knowledge of the absolute neutrino fluxes, and (ii) a 30% difference in expected rate, according to whether one takes the π^+ cross-section on a propane nucleus, or the sum of the cross-sections on the individual nucleons (see below). The large discrepancies apparent in Fig. 19 can be reduced if one selects events of $q^2 < 0.1$ GeV^2 only - see Fig 20. Any remaining discrepancy could only be demonstrated with increased statistics, allowing one to go to still smaller values of q^2. As yet, there is no disagreement with PCAC.

A related question concerns the A-dependence of the differential inelastic cross-section near $\theta_\mu = 0$[23]. In complex nuclei, the total π^+ cross-section goes as $A^{2/3}$. Does the forward neutrino cross-section also go as $A^{2/3}$, or A, like the total neutrino cross-section? A test has been made in the CERN spark chamber experiment [24], using producing layers of carbon, aluminium, iron and lead. Events were selected with $p_\mu > 1$GeV/c, and $\theta_\mu < 29^\circ$. The relative rates were consistent with an A-dependence, as expected. The Pb/C ratio was then investigated as a function of θ_μ. There was no visible dependence of the ratio on θ. However, in the "Adler region" , the errors would not positively exclude the two-fold reduction in the ratio implied by the $A^{2/3}$ law. The data are displayed in a following paper by Hahn et al.

In conclusion, one can so far make the following statements about PCAC, as tested in neutrino reactions. The region of validity of the Adler test is smaller than was originally believed, and within this region, the existing experimental data, which has large errors, is consistent with PCAC within a factor 2: this is hardly a meaningful test. The $A^{2/3}$ dependence of the forward cross-section, expected from PCAC, has not been observed, but again the errors are large in the region of small muon angles.

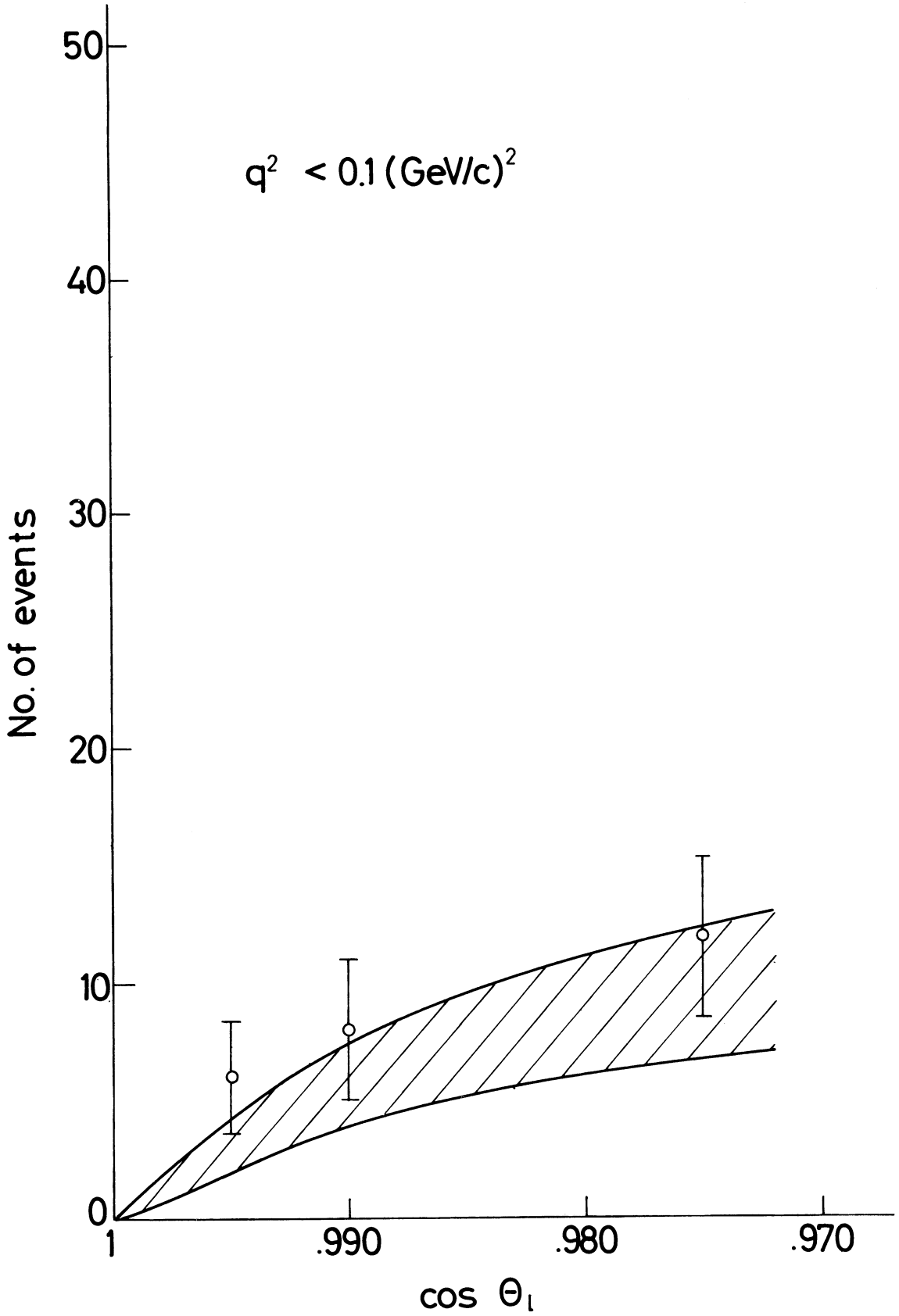

Fig.19. The observed rate of neutrino events $dN/d(\cos\theta)$, for values of θ, the angle of emission of the charged lepton, of order a few degrees. No restriction is made on q^2. The shaded region is the rate predicted from PCAC.

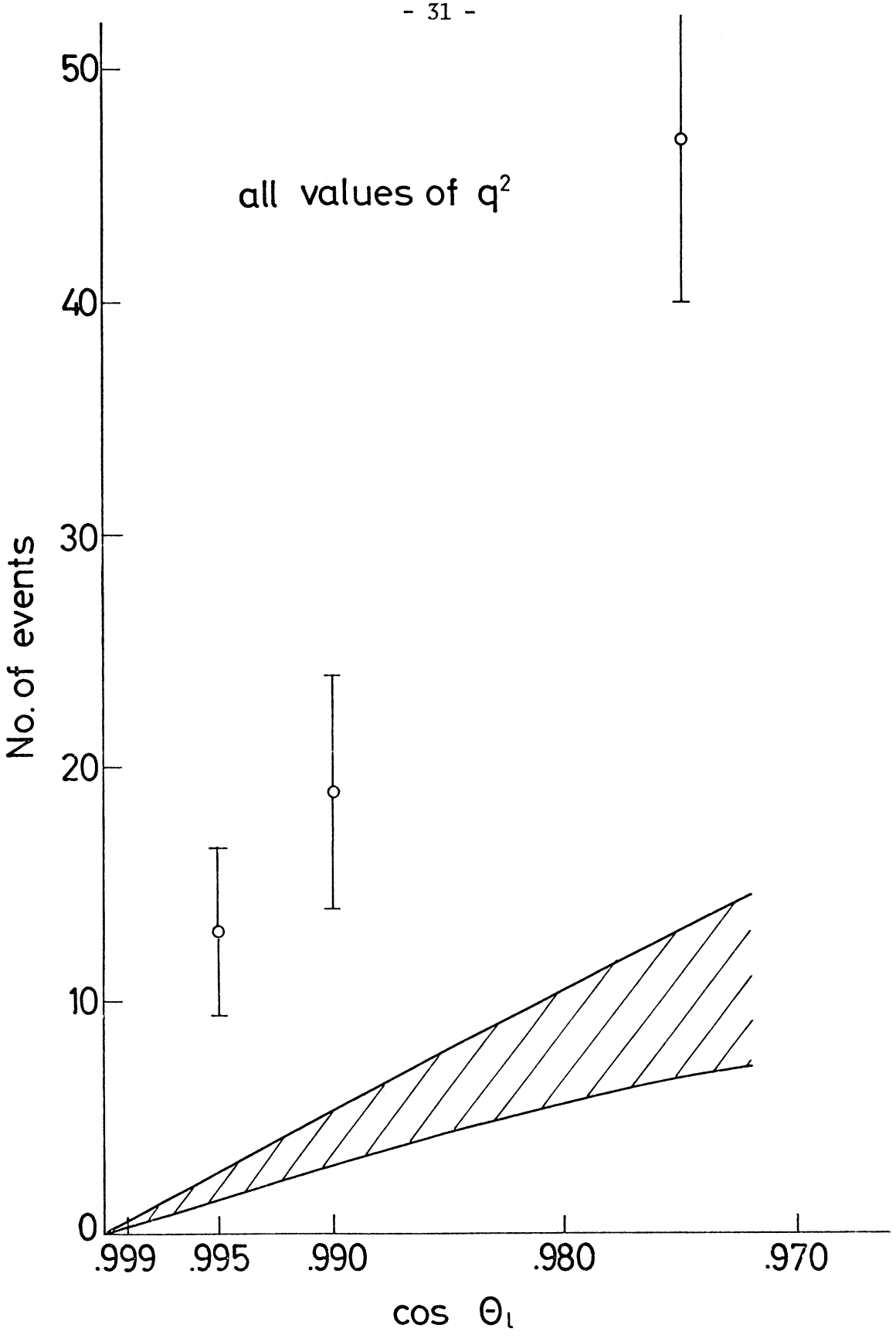

Fig.20. As in Fig. 19, for events of $q^2 < 0.1$ GeV^2.

2.4 Highly inelastic reactions.

The semileptonic processes so far discussed are concerned with phenomena in the regime of low energy/momentum transfer, and dominated by elastic and quasi-elastic scattering - the so-called resonance region.

Now we turn to the highly inelastic neutrino events, and recall some of the results obtained over the last two years or so in the parallel process of electro-production. In the high energy electron experiments - carried out mostly at SLAC - one observes only the momentum and direction of the emergent electron, and can thus deduce q^2 and the energy transfer to the nucleon, $\mathcal{E}$. The recoiling hadronic state is defined only in terms of its mass M*, through the relation

$$q^2 = M^2 - M^{*2} + 2M\mathcal{E}$$

The inelastic cross-section, assuming single photon exchange, can be written in a form due to Bjorken

$$\frac{d^2\sigma}{dq^2 d\mathcal{E}} = \left(\frac{E-\mathcal{E}}{E}\right) \frac{4\pi\alpha^2}{q^4} \cos^2\frac{\theta}{2} \left[W_2(q^2,\mathcal{E}) + 2\tan^2\frac{\theta}{2} W_1(q^2,\mathcal{E}) \right]$$

where E is the incident energy (15 GeV in these experiments), θ the direction of the secondary electron, and W_1 and W_2 are structure factors, functions of both q^2 and $\mathcal{E}$. (For the elastic case, $\mathcal{E} = q^2/2M$, so the second variable is redundant, and one recovers the Rosenbluth formula). At small θ (6° in the SLAC experiments [25]) one can suppose the second term to be small, so that one measures essentially W_2. The dependence of W_2 on q^2 and $\mathcal{E}$ - see Fig. 21 - shows the characteristic resonance behaviour at low q^2 and low $\mathcal{E}$. For $\mathcal{E} > 3$ GeV,, however, one is in the continuum region, where W_2 falls off rather slowly with $\mathcal{E}$, and where the q^2- dependence is more or less flat.

The neutrino data show, at least qualitatively, much the same sort of behaviour. Of course the number of events is small, and the experimental precision is much poorer. Fig. 22 summarizes all the neutrino bubble chamber data (in freon and propane). In freon, $\mathcal{E}$ is given, with small error, by the visible energy in hadrons, but in propane, it is necessary to make corrections

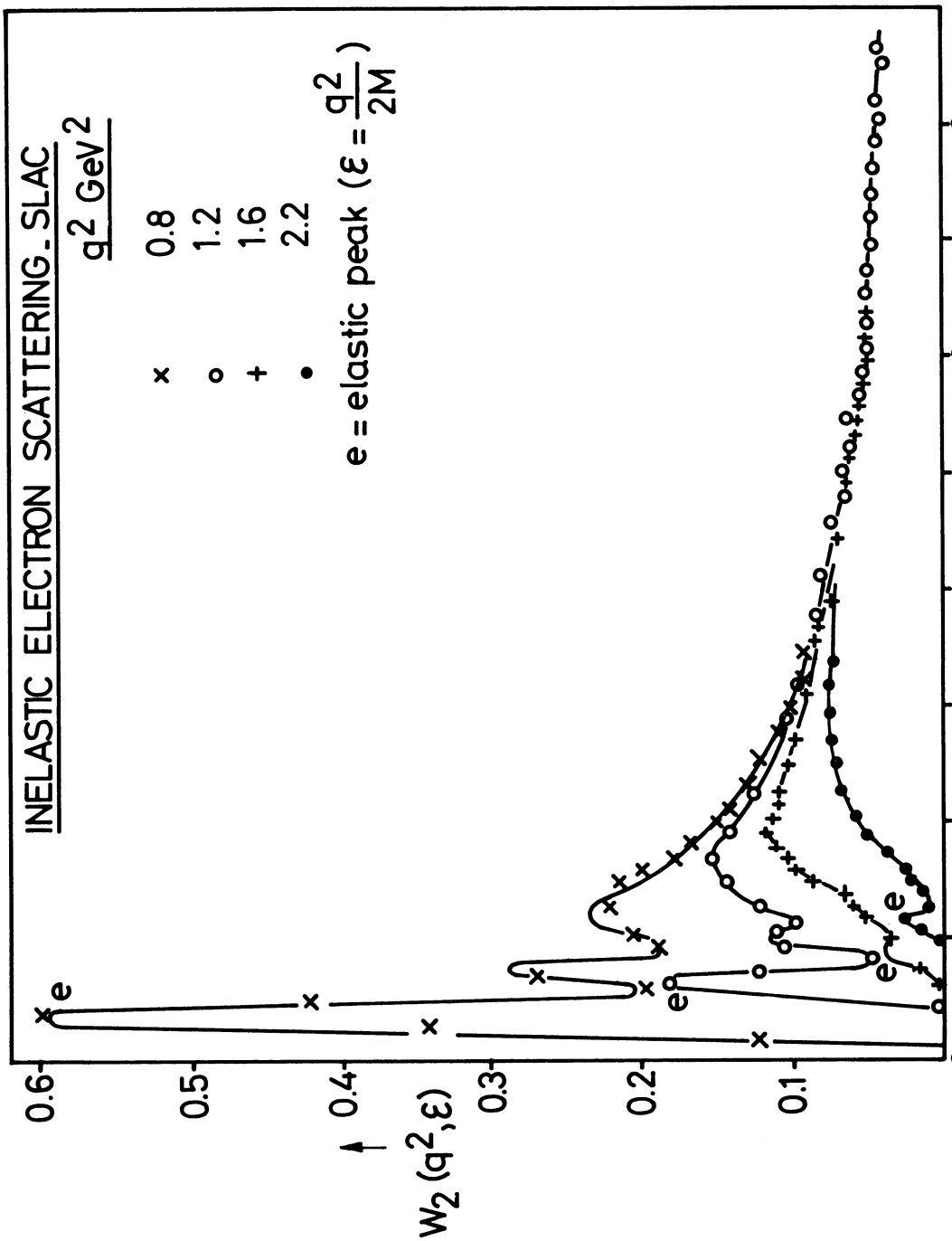

Fig.21 The electromagnetic form factor W_2 (q^2, ε) as determined in SLAC electroproduction experiments [25]. ε is the energy transfer from the electron to the nucleon, q^2 the 4-momentum transfer.

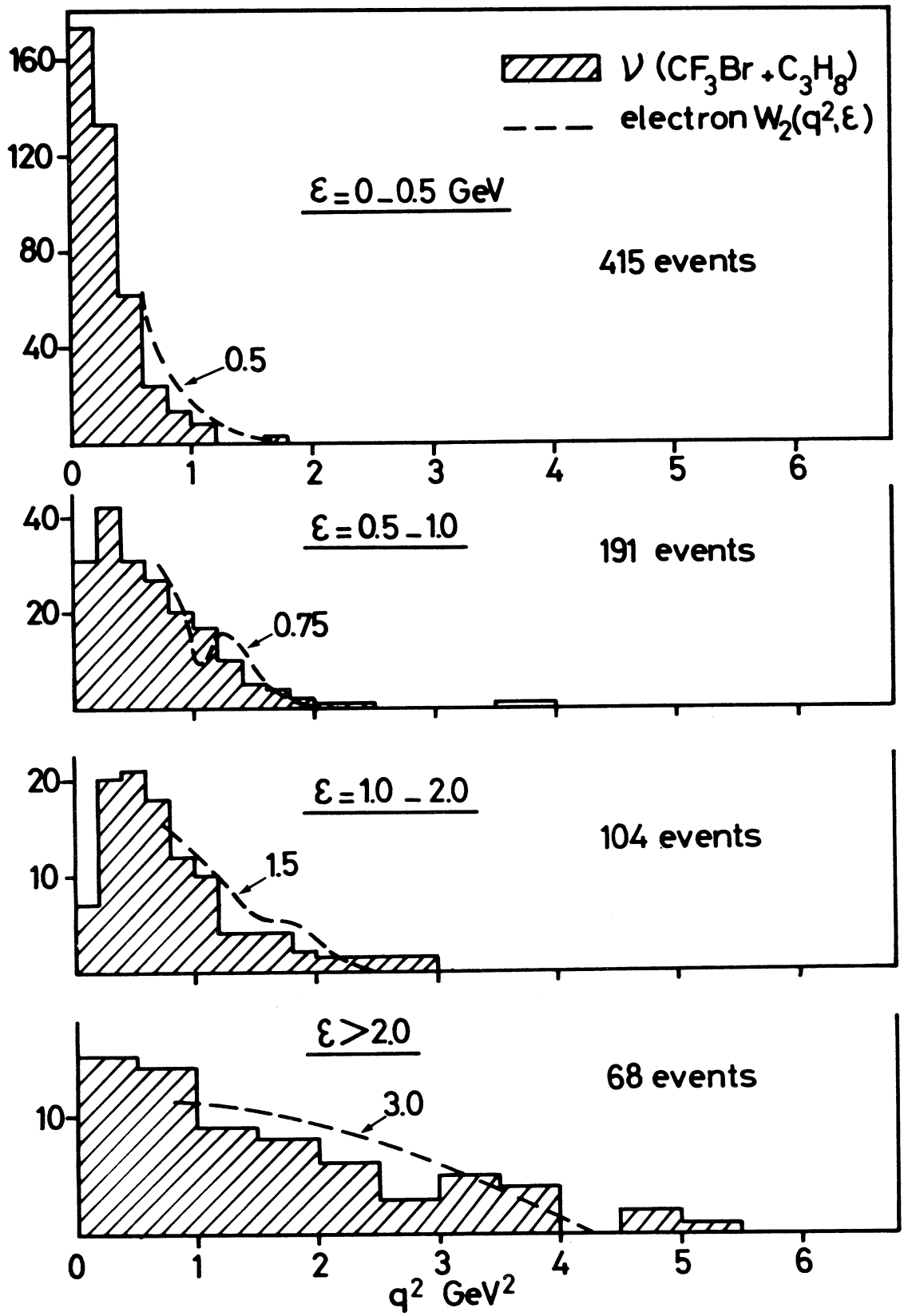

Fig.22. The q^2-distribution in neutrino bubble chamber events, for 4 regions of the energy transfer, ε. The dotted curves are taken from the data of Fig. 21, for the values of ε indicated.

(~25%) for missing energy, in the form of γ-rays, neutrons etc., escaping the chamber. The two sets of data are in good agreement when this correction is made. Another difficulty in the analysis is that, in the highly inelastic events, 2 or more negative secondaries may be observed, and the muon identification is ambiguous (in ~ 20% of events of $E_\nu > 5$ GeV). In such cases, that identification was chosen which yielded the smallest values of q^2 and/or $\mathcal{E}$.

For comparison, the shape of the electron-scattering curves (Fig. 21.) has been included (dotted lines), and one sees that the flattening out of the q^2 distribution with increasing $\mathcal{E}$ is remarkably similar in the two cases. (The electron data referred to extends only over the region $0.8 < q^2 < 2.2$ GeV^2). For the neutrino processes, it is more difficult to derive values of $d^2\sigma/dq^2\, d\mathcal{E}$, since we are dealing, not with a monoenergetic beam, but with a continuous spectrum. However, a preliminary and crude attempt at weighting the data with the incoming spectrum indicates that, within the large errors, $d^2\sigma/dq^2 d\mathcal{E}$ tends to a rather constant value for $\mathcal{E} > 2$ GeV and $q^2 < 4$ GeV^2, more or less as in the electromagnetic case.

These data suggest that, at high energies and high $\mathcal{E}$, the q^2 distribution is becoming quite flat, in other words the cross-section is like that between two point particles. This behaviour is suggested also by the sum rules derived from current algebra. For example, Adler[26] has derived the following sum rules, at infinite neutrino energy, for the total cross-sections on nucleons:-

$$\frac{d\sigma\,(\bar{\nu}p)}{dq^2} - \frac{d\sigma\,(\nu p)}{dq^2} \underset{E_\nu \to \infty}{=} \frac{G^2}{\pi}\,(\cos^2\theta_c + 2\sin^2\theta_c)$$

and $$\frac{d\sigma\,(\bar{\nu}n)}{dq^2} - \frac{d\sigma\,(\nu n)}{dq^2} \underset{E_\nu \to \infty}{=} \frac{G^2}{\pi}\,(-\cos^2\theta_c + \sin^2\theta_c)$$

where θ_c is the Cabibbo angle. The input for these sum rules is (a) locality of the lepton current (b) the commutation relations of the hadron currents (c) the assumption that one amplitude satisfies an unsubtracted dispersion

relation. One sees that the difference in the particle and antiparticle cross-sections is a constant, i.e. a point-like cross-section ($\cos^2\theta_c + 2\sin^2\theta_c \simeq 1$, and G^2/π is just the differential cross-section for S-wave neutrino-electron scattering). There are similar sum-rules for electron-nucleon scattering [27].

Another, and quite different way to arrive at point-like cross-sections is to postulate point-like constituents in the nucleon.[28] These constituents can be imagined as "bare" quarks - if anyone can imagine such objects. Then elastic neutrino scattering results from coherent scattering of the lepton off all 3 quarks. At much higher q^2, the scattering is mostly incoherent, and one obtains highly complex inelastic processes; yet if one sums over all elastic plus inelastic channels, the total cross-section will be given by the elementary lepton-quark elastic cross-section, i.e. $d\sigma/dq^2$ = constant. The constant factors in the Adler sum rules would then be interpreted in terms of the constant difference in the number of constituents with isospin up and down respectively (since, for example, a neutrino, transforming to μ^-, could only be scattered by an isospin - down constituent). This model is almost unbelievably crude, and, as Gottfried has remarked, no well educated person should be expected to accept it. Yet it at least has the virtue of making rather definite predictions. For example, the form-factors for the elastic and quasi-elastic processes should be all the same, and simply the Fourier transform of the quark distribution. One also gets simple predictions like

$$\sigma^{\text{total}}(\nu n) = 2\,\sigma^{\text{total}}(\nu p)$$
$$(E_\nu \to \infty,\ q^2 \to \infty)$$

which should be fairly easy to verify in the near future, provided infinity is not too far away.

A third point of view is that the high energy, highly inelastic region is dominated by diffractive processes, and Stodolsky has contributed a paper on the theme at this conference. In the energy region up to $E_\nu \sim 10$ GeV,

however, the indications are that the computed rates for diffractive production of vector mesons contribute only a few per cent of the total cross-section †.

2.5 Total Cross-Section

Fig. 23. shows preliminary data on total neutrino cross-sections observed in freon and propane. The propane data has been corrected for missing energy, as described earlier - this results in an average 10% increase to the total visible energy. The freon data is the raw data, since any correction is very small. The neutrino spectrum in the propane runs was quite well determined, from muon spectrum measurements. In the earlier runs with freon filling however, the spectrum is only known from "dead-reckoning", using yield data on pion and kaon production from thin targets. The agreement between the two sets of data is encouraging but might be accidental.

The indications from these results are that the total neutrino cross-sections are still rising steadily, at the highest energies presently accessible. For a linear energy dependence, the coefficient is approximately

$$\sigma_{total} \simeq 0.6\ E_\nu \quad (\text{units } 10^{-38}\ \text{cm}^2/\text{nucleon}, E_\nu \text{ in GeV})$$

One might remark that the constituent model would also predict a linear dependence, however with a coefficient ~ 1.4.

It is clear that future investigations of the dependence of total cross-section on neutrino energy will be of the greatest importance to our understanding of the highly inelastic processes. With a narrow-band neutrino beam at the 200/400 GeV machine, for example, such an experiment could be done with an extremely crude spark chamber array, since one is interested only in good identification of the muon and the total event rate.

A further spin-off from such measurements relates to the local nature of the leptonic current. All the discussion above has been in terms of such locality. As pointed out many years ago by Pais [29] and by Lee and

---

† See also the paper by B. Roe on diffractive ρ- production at this conference.

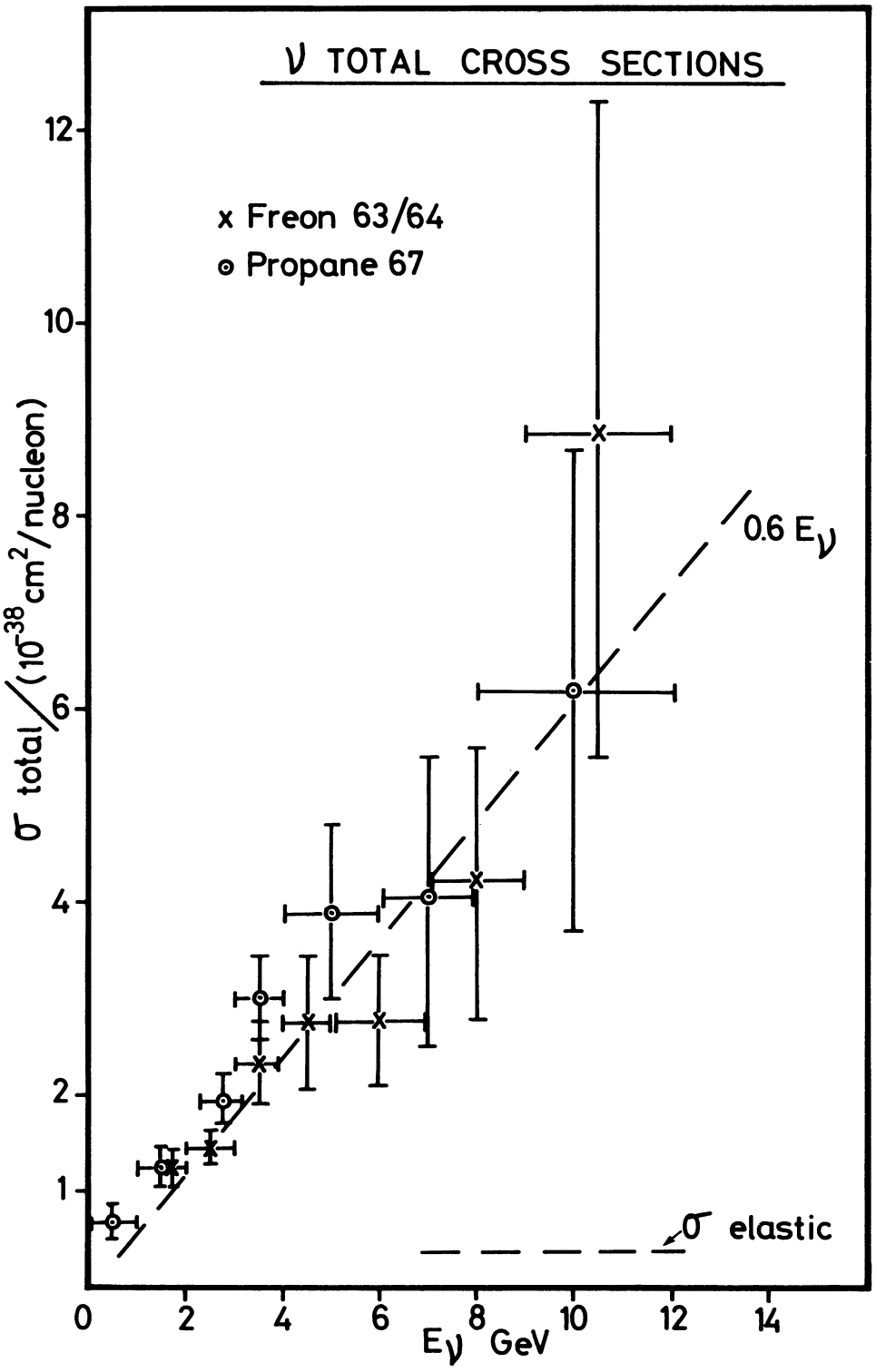

Fig.23 The total neutrino cross-sections as a function of neutrino energy, for the CERN bubble chamber data. As in Fig. 22, about half the events are from the freon runs (1963/4) and the rest from the propane run (1967).

Yang[30], such an assumption implies that the cross-section must have the form

$$\frac{d^2\sigma}{dq^2\, d\mathcal{E}} = \frac{A}{E_\nu^2} + \frac{B}{E_\nu} + C$$

i.e. they can be at most quadratically dependent on neutrino energy. A, B, and C are structure factors, $A = A(q^2, \mathcal{E})$ etc. If, as everyone suspects, the locality hypothesis eventually breaks down, one would obtain a more complicated dependence, and the result would be that the steady rise in cross-section would be halted - and presumably flatten off.

So, the inelastic processes are highly interesting from two distinct points of view. One is that emphasized in the previous section, the possibility of digging into the fundamental structure of the hadrons. The other is that, especially if the hadronic currents have a point-like component, one can use nucleon targets as tools to hammer away at the lepton vertex in the region of extremely high q^2, and perhaps find something equally fundamental about the purely leptonic processes.

2.6 Future Neutrino Event Rates.

I have so far said nothing about the technical aspects of neutrino experiments. Fig. 24. is taken from a paper by Dr. C. A. Ramm given at the neutrino conference yesterday. It is self-explanatory, and shows that, over the years, the tremendous advances in neutrino beam technology, improvements in machine intensity and energy, and the construction of ever bigger detectors, has led and will lead to an exponential growth in neutrino event rates. The first and, so far, the only major discovery in this field came in 1961 (at the very bottom of the curve) with the observation of the two types of neutrino by the Columbia/BNL group - based on a dozen or so events. We are now nearly half-way up the curve, without any real sign of a comparable break-through, but still there are a few orders of magnitude in hand.

2.7 Acknowledgements

It is a pleasure to acknowledge the invaluable help of the personnel of the CERN, NPA Division in preparing this report, and for allowing me access to much of their unpublished data.

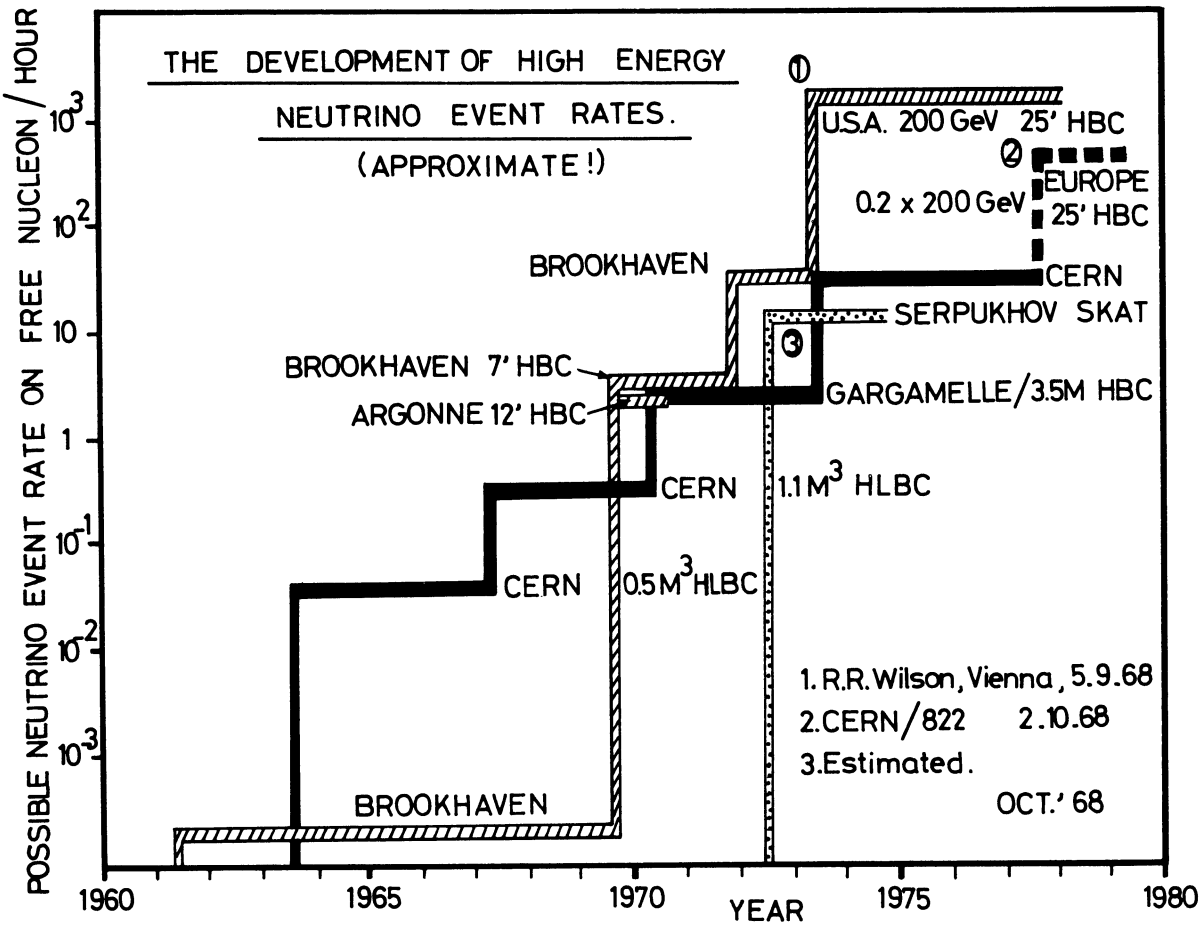

Fig.24. Neutrino event rates as a function of time, for various accelerators and detectors.

REFERENCES

1) K. Borer, B. Hahn, H. Hofer, H. Kaspar, F. Krienen, T.-G. Seiler Proc. Vienna Conf. on El. Particles (Sept. '68)

2) G. Bernardini et al Phys. Lett. 13, 86 (1964)

3) R. Burns et al Phys. Rev. Lett. 15, 830 (1965)

4) A. C. T. Wu, C. P. Yang, K. Fuchel and S. Heller. Phys. Rev. Lett. 12, 57 (1964)

5) S. L. Glashow, H. J. Schnitzer and S. Weinberg. Phys. Rev. Lett. 19, 205 (1967)

6) R. N. Mohapatra, S. J. Rao and R. E. Marshak. Phys Rev. Lett. 20, 108 (1968)

7) M. Gell-Mann, M. L. Goldberger, N. M. Kroll and F. E. Low. Proc. Vienna Conf. on El. Particles. (September 1968)

8) W. Czyz, G. C. Sheppey and J. D. Walecka. Nuov. Cim. 34, 404 (1964)

9) H. Yoshiki, private communication (1969). (Preliminary data (1965) was presented by H. Yoshiki, CERN NPA/Int. 64-40 and C. Franzinetti, CERN NPA 66-13 (1966).)

10) M. M. Block et al, Phys. Lett. 12, 281 (1964); D. C. Cundy, Proc. ANL Conf. on Weak Int. ANL-7130, p. 257 (1965)

11) J. Lovseth, CERN TH 861 (1967).

12) M. Holder et al Nuov. Cim. 57, 338 (1968)

13) S. M. Berman and M. Veltman. Nuov. Cim. 38, 993 (1965)

14) R. L. Kustom, D. E. Lundquist, T. B. Novey, A. Yokosawa, and F. Chilton ANL preprint (1969).

15) CERN NPA group, in course of publication.

16) I. Budagov et al Proc. Vienna Conf. on El. Particles (Sept. '68)

17) Ph. Salin. Nuov Cim. 48, 506 (1967) see also; G. Altarelli, R. Gatto and G. Preparata. Nuov. Cim. 37, 1817 (1965)

18) S. L. Adler; Annals of Physics (in press).

19) S. L. Adler. Phys. Rev. 135, B 963 (1964)

20) J. Bartley and C. Franzinetti CERN/NPA Int. 65-14 (1965)

21) C. Franzinetti CERN/NPA 66-13 (1966)

22) S. Bonetti et al Proc. Vienna Conf. on El. Particles (Sept '68)

23) J. S. Bell. Phys Rev. Lett. 13, 57 (1964)

24) Hahn et al; Proceedings of this Conference.

25) W. Panofsky; Proc. Vienna Conf. on El. Particles (Sept '68)

26) S. L. Adler. Phys Rev. 140, B736 (1965) Phys. Rev. 143 1144 (1966)

27) J. D. Bjorken, Phys. Rev. Lett. 16, 408 (1966)

28) K. Gottfried Phys. Rev. Lett. 18, 1174 (1967)

29) A. Pais. Phys. Rev. Lett. 9, 117 (1962)

30) T. D. Lee and C. N. Yang Phys. Rev. 126, 2239 (1962)